Disease Models & Mechanisms 4, 67-85 (2011) doi:10.1242/dmm.005561

Transmembrane potential of GlyCl-expressing instructor cells induces a neoplastic-like conversion of melanocytes via a serotonergic pathway

Douglas Blackiston[1,2], Dany S. Adams[1], Joan M. Lemire[1], Maria Lobikin[1] and Michael Levin[1,*]

SUMMARY

Understanding the mechanisms that coordinate stem cell behavior within the host is a high priority for developmental biology, regenerative medicine and oncology. Endogenous ion currents and voltage gradients function alongside biochemical cues during pattern formation and tumor suppression, but it is not known whether bioelectrical signals are involved in the control of stem cell progeny in vivo. We studied *Xenopus laevis* neural crest, an embryonic stem cell population that gives rise to many cell types, including melanocytes, and contributes to the morphogenesis of the face, heart and other complex structures. To investigate how depolarization of transmembrane potential of cells in the neural crest's environment influences its function in vivo, we manipulated the activity of the native glycine receptor chloride channel (GlyCl). Molecular-genetic depolarization of a sparse, widely distributed set of GlyCl-expressing cells non-cell-autonomously induces a neoplastic-like phenotype in melanocytes: they overproliferate, acquire an arborized cell shape and migrate inappropriately, colonizing numerous tissues in a metalloprotease-dependent fashion. A similar effect was observed in human melanocytes in culture. Depolarization of GlyCl-expressing cells induces these drastic changes in melanocyte behavior via a serotonin-transporter-dependent increase of extracellular serotonin (5-HT). These data reveal GlyCl as a molecular marker of a sparse and heretofore unknown cell population with the ability to specifically instruct neural crest derivatives, suggest transmembrane potential as a tractable signaling modality by which somatic cells can control stem cell behavior at considerable distance, identify a new biophysical aspect of the environment that confers a neoplastic-like phenotype upon stem cell progeny, reveal a pre-neural role for serotonin and its transporter, and suggest a novel strategy for manipulating stem cell behavior.

INTRODUCTION

It is now clear that misregulation of stem cell fate and division is an important component of neoplasia (Gonzalez, 2007). Some tumors (at least in the case of blood, breast, skin, brain and colon cancer) might originate from malignant transformation of stem cells (Hess et al., 2007; Kyrgidis et al., 2010; Lee et al., 2005; Reya et al., 2001). Moreover, because cancer development fundamentally involves the loss of morphogenetic order (Lee and Vasioukhin, 2008; Levin, 2009b; Oviedo and Beane, 2009), it is not surprising that the same signaling pathways (TGFβ, Wnt, Notch, etc.) seem to regulate self-renewal in embryonic patterning, stem cells and cancer cells (Al-Hajj et al., 2004; Bjerkvig et al., 2005; Hong et al., 2008; Reya et al., 2001; Wicha et al., 2006). Developmental systems serve as convenient models for studies of cancer because they allow access to a number of stem cell populations throughout embryogenesis and benefit from well-documented regulatory networks that underlie differentiation and patterning. Perturbations that induce neoplasia-like phenotypes during embryogenesis allow great insight into the signals leading to the creation of cancer stem cells and many such links have already been established (Domen et al., 1998; Domen and Weissman, 2000; Taipale and Beachy, 2001; Varnum-Finney et al., 2000).

Thus, stem cells are at the center of the regeneration-development-cancer triad (White and Zon, 2008). The construction of replacement tissues or organs through stem cell therapy or in vitro bioengineering is a fundamental hope of regenerative medicine. Although much effort is directed towards coaxing stem cells to differentiate into specific cell types, the next frontier will involve learning to harness individual cellular dynamics to achieve complex multicellular morphogenesis. Building replacement organs or whole appendages to address birth defects, tumors, degenerative disease, injury and infectious morbidity will require not merely the presence of the right cell types, but also their integration into three-dimensional highly complex structures of appropriate physiological and mechanical function (Ingber and Levin, 2007). This in turn will require a detailed understanding of the role of the cellular environment of the host in regulating the behavior of stem and cancer cells alike (Ingber, 2008; Soto and Sonnenschein, 2004).

The neural crest, a crucial population of embryonic stem cells that contributes to many structures during development (Sauka-Spengler and Bronner-Fraser, 2008), differentiates into a variety of cell types, including smooth muscle cells, peripheral neurons and glia, and craniofacial cartilage and bone, as well as endocrine and pigment cells. The biology of neural crest regulation is also of significant biomedical relevance because neurocristopathies form an important class of birth defects (Bergstrom et al., 2005; Bolande,

[1]Center for Regenerative and Developmental Biology, and Biology Department, 200 Boston Avenue, Suite 4600, Tufts University, Medford, MA 02155, USA
[2]Department of Regenerative and Developmental Biology, Forsyth Institute, Boston, MA 02115, USA
*Author for correspondence (michael.levin@tufts.edu)

Received 12 February 2010; Accepted 23 August 2010

1997; Inoue et al., 2007). These cells are an ideal context in which to explore the common mechanisms regulating stem cells and neoplastic processes (Crane and Trainor, 2006; Fuchs and Sommer, 2007; Tucker, 2004), especially with respect to pigment cell derivatives (Cooper and Raible, 2009; White and Zon, 2008). These cells not only reveal dynamics of migration control (Kuriyama and Mayor, 2008; Macmillan, 1976), but are also an important subject for understanding melanoma (Haass and Herlyn, 2005; Haass et al., 2005) and in learning to control biological assembly in vitro for tissue engineering (Maniotis et al., 1999).

One of the most interesting areas of inquiry involves epigenetic controls of tumor progression and stem cell function (Baylin and Ohm, 2006; Bulic-Jakus et al., 2006; Ducasse and Brown, 2006; Jaffe, 2003; Park et al., 2007; Rubin, 1990; Welsch et al., 2007). It is becoming clear that the microenvironment is a key player that mediates epigenetic signaling mechanisms (Bissell and Labarge, 2005; Hendrix et al., 2007; Soto and Sonnenschein, 2004; Uzman et al., 1998). Importantly, it is now known that cell behaviors are controlled not only by secreted chemical factors, traction forces and extracellular matrix, but also by bioelectrical events. Ionic controls of differentiation, proliferation and migration have been investigated for decades (Borgens et al., 1989; Jaffe, 1982; Lund, 1947; Nuccitelli et al., 1986; Robinson and Messerli, 1996), with solid functional data demonstrating instructive roles in growth control, limb regeneration and anterior-posterior polarity. More recently, the investigation of bioelectric signals has been accelerated by the availability of high-resolution molecular-genetic tools allowing the functional dissection of the endogenous roles of ion flows, voltage gradients and electric fields, and their linkage to canonical genetic and biochemical networks (Adams and Levin, 2006a; Adams and Levin, 2006b; Adams et al., 2007; Reid et al., 2007; Song et al., 2007; Zhao et al., 2006). Indeed, voltage- and current-mediated signals are now known to carry morphogenetic information, including signals regulating embryonic left-right patterning, wound healing and neuromuscular appendage regeneration (Levin, 2007; Levin, 2009a; McCaig et al., 2005; McCaig et al., 2009), as well as controlling cell-level behaviors such as cell migration and proliferation (Blackiston et al., 2009; Pullar et al., 2006; Rajnicek et al., 2006; Sundelacruz et al., 2009).

It is known that transmembrane voltage is a powerful determinant of proliferative potential in somatic cells (Binggeli and Weinstein, 1986; Blackiston et al., 2009; Cone and Cone, 1976; Olivotto et al., 1996); moreover, genomic analyses and microarray screens have now revealed a number of ion channels to be key players in neoplasm (Arcangeli, 2005; Arcangeli et al., 2009; Fraser et al., 2005). Recent studies have shown that stem cells exhibit unique electrophysiological profiles (Biagiotti et al., 2006; Cai et al., 2004; Gersdorff Korsgaard et al., 2001; Heubach et al., 2004; van Kempen et al., 2003). Likewise, ionic currents and channels have been found to play important roles during myoblast, cardiomyocyte, mesenchymal and neural stem cell differentiation (Biagiotti et al., 2006; Cho et al., 2002; Konig et al., 2004; Sun et al., 2005; Sundelacruz et al., 2008; van Kempen et al., 2003).

However, much of this work was done in vitro, which does not reveal the complex interactions that are required to integrate stem cell function into complex morphogenetic programs. Thus, the ability of endogenous electrical signals to act as a functional biophysical control mechanism in stem cell biology in vivo is very poorly understood. Recently, in the *Xenopus laevis* embryonic system, we showed that misexpression of a regulatory subunit of the KCNQ1 potassium channel was able to induce hyperproliferation of melanocytes and a hyperpigmented phenotype that did not involve increases of pigment content per cell or the conversion of other cell types into melanocytes (Morokuma et al., 2008). This work revealed an entirely novel control of melanocyte behavior and led to several new questions. First, because misexpression of channel mRNA must be performed at cleavage stages, the timing of the melanocyte-instructive event could not be functionally characterized. Second, for the purposes of using bioelectrical controls of cell behavior for regenerative medicine or oncology, it is essential to develop techniques that do not rely on the introduction of transgenes because of the numerous problems attendant with gene therapy in human patients (Pfeifer and Verma, 2001; Thomas et al., 2003). Third, it is not known which cells, in what anatomical region, must be depolarized for the melanocytes to acquire the metastatic phenotype. Finally, it is not known what cells in the embryo endogenously have the ability to signal to neural crest descendants when their membrane voltage potential (V_{mem}) is modulated, nor whether the KCNE1-induced signaling could be exerted by proteins other than the KCNE1-KCNQ1 potassium channel complex.

Therefore, we developed a strategy capitalizing on the ability to control the native glycine receptor chloride channel (GlyCl), and thereby control the steady-state transmembrane potential of GlyCl-expressing embryonic cells. Molecular-genetic or pharmacological depolarization of GlyCl-expressing cells confers a neoplasia-like phenotype on melanocytes: they overproliferate, become arborized and inappropriately colonize numerous tissues in a metalloprotease-dependent fashion. A similar effect is observed in cultured human melanocytes. The effect is specific to V_{mem} (not dependent on GlyCl per se or even chloride flux), is not cell-autonomous and is mediated by voltage control of serotonin [5-hydroxytryptamine (5-HT)] transport. These data (1) identify GlyCl as a unique marker of cells that can control melanocyte behavior non-cell-autonomously, (2) reveal a novel mechanism by which bioelectrical properties of the microenvironment mediate the stem-cell–cancer-cell transition and (3) suggest a new class of strategies for manipulating embryonic stem cell behavior without the need for gene therapy.

RESULTS

Exposure to chloride channel opener specifically induces hyperpigmentation

To investigate the role of bioelectric signals during embryogenesis and develop a strategy that could ultimately be used in biomedical settings, we first developed a method for modulating transmembrane potential in select groups of cells in vivo. Chloride channels are a convenient target because, once opened, Cl^- ions can be made to exit or enter the cell when the extracellular level of chloride ($[Cl^-]_{ex}$) in the medium is artificially varied (Lerchner et al., 2007): levels of $[Cl^-]_{ex}$ that are lower than that of intracellular chloride will lead to the exit of negative ions and thus depolarize the cells. Conversely, a high chloride medium will cause hyperpolarization by allowing negative ions to enter cells down their concentration gradient. To open chloride channels, we utilized ivermectin – a drug commonly used as an antiparasitic agent owing

to the paralyzing effect it has on muscle cells in nematodes (Ottesen and Campbell, 1994). This compound is well-characterized, specifically opening GlyCl, and is already approved for use in human patients and veterinary medicine (Shan et al., 2001).

Untreated wild-type *Xenopus* embryos develop characteristic pigment patterns after a fraction of neural crest derivatives become determined as melanocytes during late neurulation and somite stages (Collazo et al., 1993; Kumasaka et al., 2005) and begin to produce melanin during tailbud stages. The majority of melanocytes occupy a medial position in the head and trunk of young tadpoles (Fig. 1A,A′). *Xenopus* developing in 0.1× Modified Marc's Ringers (MMR) medium, [Cl^-]=10 mM {lower than internal Cl^- concentration ($[Cl^-]_{int}$), which is 40-60 mM}, were exposed to 10 μM ivermectin, which, under these conditions, is a depolarizing agent affecting cells that express GlyCl (supplementary material Fig. S1). Treatment throughout development from early neurulation paralyzed older tadpoles, as expected from the depolarization effect. Strikingly, it also resulted in extensive hyperpigmentation. Melanocytes in treated individuals often migrated to regions normally devoid of pigment cells, such as the lateral eye field (Fig. 1B, red arrows) and the dorsal and ventral fins (Fig. 1B″,B‴), and filled the core of the tail (Fig. 1B′). This phenotype occurred in 98% of treated larvae (Fig. 1C; supplementary material Movies 1 and 2); importantly, however, development was otherwise normal. Embryos showed no differences in growth rate or morphogenesis compared with wild type, and had a normal dorsoanterior index in addition to proper patterning of the body axis and organs. Other neural-crest-derived organs such as the branchial arches were apparently normal, arguing against significant deviation of neural crest streams from other targets. We conclude that pharmacological opening of chloride channels in embryos specifically results in hyperpigmentation.

Ivermectin-induced hyperpigmentation involves inappropriate migration, ectopic colonization and cell shape change

To determine whether the hyperpigmentation was due to migration of melanocytes to inappropriate locations, and whether this process, like metastasis, depends on metalloproteases (MMPs), we treated embryos with a combination of ivermectin and the well-characterized MMP inhibitor NSC-84093, which blocks melanocyte movement in frog embryos (Tomlinson et al., 2009a; Tomlinson et al., 2009b). The resulting embryos (Fig. 1D,D′) exhibited hyperpigmentation in regions normally inhabited by melanocytes (above the neural tube) but revealed an absence of ectopic melanocytes in periocular locations (Fig. 1D, yellow arrows). We conclude that ectopic melanocytes colonize inappropriate embryonic regions via MMP-dependent cell migration processes. Interestingly, the melanocytes did not colonize the area above the pineal gland (Fig. 1B,D, blue arrow), suggesting that they might still be responsive to specific restrictive signals that can demarcate quite sharp boundaries between permitted and restricted regions. We attempted to recapitulate this effect and restrict the metastatic melanocytes from other regions by inducing foci of high melatonin, but this was unsuccessful, suggesting that the repulsive effect of the pineal is not due exclusively to melatonin (data not shown).

One important component of the phenotype was a notable increase in cell arborization (Fig. 1A′ vs Fig. 1B′ and Fig. 2; see

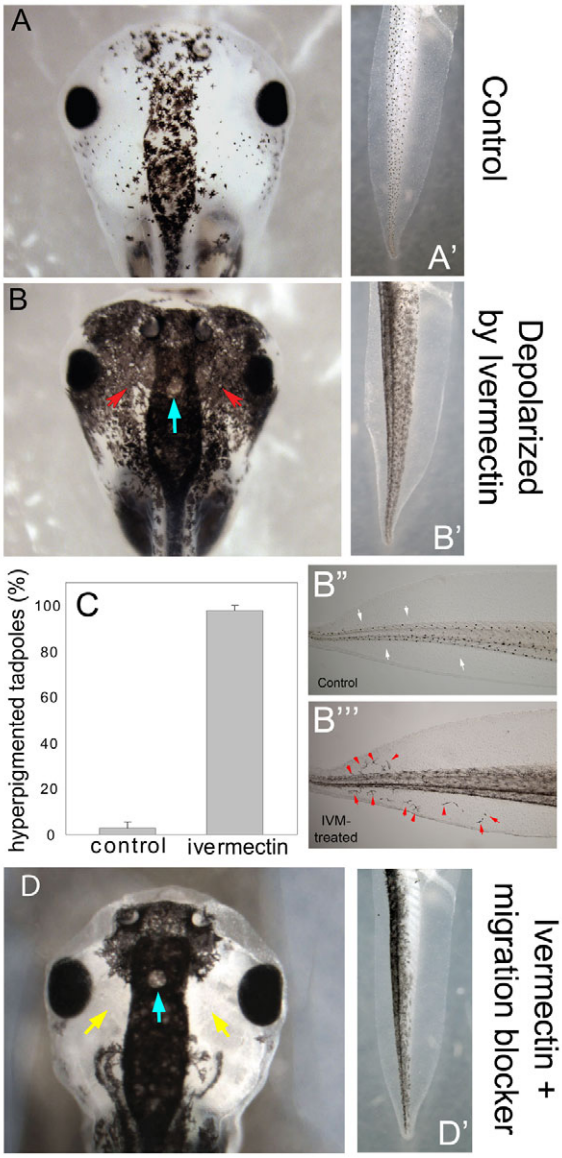

Fig. 1. Ivermectin exposure induces hyperpigmentation. (A) Control embryos display a medially concentrated pigment pattern with the lateral eye field being largely devoid of melanocytes. (A′) The tail normally has a distributed population of round melanocytes over its core. (B) Embryos exposed to the chloride channel activator ivermectin while developing in the normal 10 mM Cl^- medium acquire a hyperpigmented phenotype by stage 42 despite otherwise normal development; ectopic melanocytes are present (periocular region indicated by red arrows; compare to similar region in panel A), and (B′) are more numerous and spread out in the tail. Ectopic melanocytes are also found in the dorsal and ventral fins (compare B‴ to control tails in B″). White arrows indicate fin region normally devoid of melanocytes; red arrowheads indicate ectopic melanocytes. (C) The ivermectin-induced phenotype was highly penetrant, with 98% of treated embryos developing hyperpigmentation (error bars indicate one standard deviation, *n*=189 for controls, *n*=174 for ivermectin-exposed). (D) When migration was blocked by the MMP inhibitor NSC-84093 in ivermectin-exposed embryos, colonization of ectopic locations by melanocytes was prevented (yellow arrows) but the abnormal arborization remained. The effect was also observed in the tail (D′), with the ventral area remaining uncolonized. Blue arrow indicates the location of an area that remains free of ectopic melanocytes, even in heavily hyperpigmented tadpoles, possibly overlying the pineal gland.

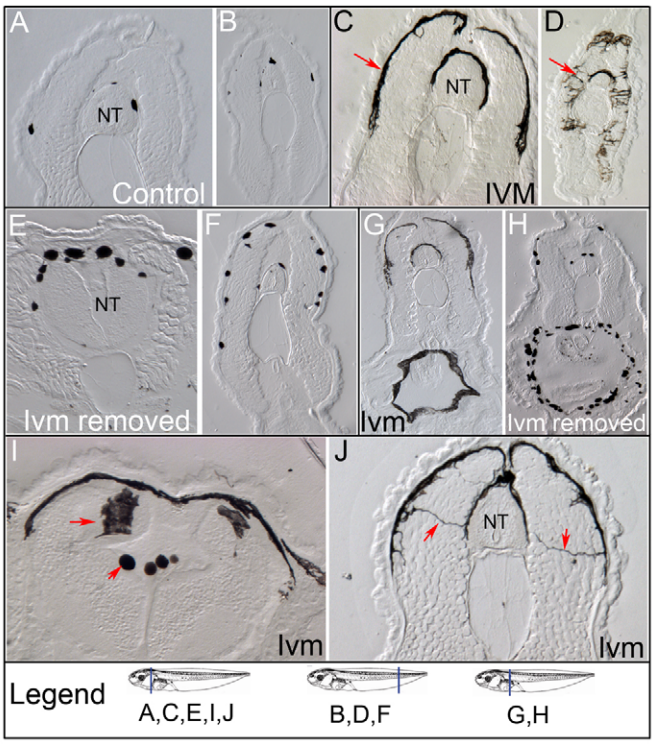

Fig. 2. Ivermectin induces invasiveness in melanocytes. Compared to control embryos (A,B), those exposed to ivermectin (IVM) throughout development (C,D) show significantly more melanocyte coverage of the neural tube (NT) and epidermis (red arrows). Ivermectin-treated embryos removed from ivermectin at stage 43 (E,F) still show increased pigment cell number compared with controls, but the cells lose their arborized phenotypes. In addition, ivermectin induces melanocyte colonization of the gut (G,H) and the interior of the neural tube (I), and invasiveness of projections throughout the mesoderm between the epidermis and neural tube (J), indicated by red arrows. Schematics of *Xenopus laevis* embryo stages were retrieved from Xenbase, University of Calgary, Alberta T2N 1N4, Canada; http://www.xenbase.org/; August 2010.

supplementary material Fig. S1F and its legend for evidence that pigment pattern is a reliable indicator of overall shape in melanocytes). The arborization remained despite MMP inhibition (Fig. 1D,D′), suggesting that the hyperpigmentation is due not only to melanocytes being present in ectopic locations, but also to a separate process involving shape change. This was clearly apparent in sections of hyperpigmented tadpoles, which revealed extensive tissue occupation by ectopic melanocytes. In sections, wild-type animals typically have sparse pigmentation along the lateral epidermis and around the neural tube (Fig. 2A,B), exhibiting only a small number of round melanocytes. Ivermectin-exposed hyperpigmented embryos instead possess dramatic melanocyte coverage around the majority of the epidermis and the neural tube (Fig. 2C,D), which includes the change of cells from a rounded morphology to a spread-out highly arborized shape with long processes.

We next investigated whether the effect was reversible. Embryos removed from ivermectin-containing medium at stage 43 (after melanocytes had migrated) and analyzed 2 days later also showed an increase in melanocyte number compared with controls but did not maintain the abnormal arborization (Fig. 2E-H). We conclude that the arborized phenotype is reversible; however, the ectopic melanocytes remain once they colonize the region.

The migratory properties of these ectopic melanocytes were extensive. They colonized not only the lumen of the neural tube, but also penetrated the dense neural tissues (Fig. 2I). They also sent very long projections from the edges of the somite into the neural tube (Fig. 2J). We conclude that depolarization via chloride channel opener induces aberrant targeting and a high degree of migration while radically changing the normal morphology of melanocytes – a phenotype that is reminiscent of metastasis.

Early ivermectin exposure results in an increased number of melanocytes

We next investigated whether the hyperpigmentation effect involves increased numbers of melanocytes, in addition to ectopic migration and shape change. Exposed embryos were anesthetized and photographed; we then counted the number of melanocytes within a standard region defined by the eyes (Fig. 3A,B), and compared each treatment to age-matched control siblings. Embryos exposed to 10 μM ivermectin from stages 12-24 (gastrulation through to the completion of neurulation), washed three times and cultured in plain 0.1× MMR, show a 1.5-fold increase in melanocyte number compared with controls (Fig. 3C; ANOVA Tukey post-hoc, $P<0.05$). These results were not confined to the eye field: melanocyte counts in the tip of the tail also showed a significant 1.5-fold increase when exposed to ivermectin throughout development (Student's *t*-test, $t=6.069$, $P\leq0.001$). Importantly, we detected no increase in total melanin content above that explained by the increase in cell number (absorption at 414 nm: control=0.0534, ivermectin-treated=0.0656, $n=5$ embryos per treatment, repeated five times, 1.2-fold difference); because the increase in melanocyte number (1.5-fold) is bigger than the increase in melanin content, each melanocyte is actually less pigmented in ivermectin-exposed tadpoles, ruling out higher pigment synthesis as a contributing factor to the hyperpigmented appearance.

Excess melanocytes can arise from increases in proliferation, change of cell fate of additional cells into melanocytes, or perhaps even failure of apoptosis. Quantification of cells positive for caspase-3 staining (Tseng et al., 2007) in sections showed no significant difference between control and ivermectin-treated embryos (11.3 vs 10.2 apoptotic cells in the notochord of control vs ivermectin-treated embryos, respectively, $n=11$, $P=0.6$), ruling out prevention of programmed cell death as a likely reason that higher numbers of melanocytes are observed. We next investigated whether additional cells were being recruited towards a melanocyte fate by expression analysis of *Trp2* (also known as *Dct*), a definitive marker of mature melanocytes (Kumasaka et al., 2003). Embryos treated with ivermectin from stage 11 that were examined for expression of *Trp2* at stage 28 (prior to the migration of pre-melanocytes away from the neural crest) showed no ectopic signal (Fig. 3D,E), indicating that regions that later exhibit abnormal numbers of melanocytes do not do so because of any recruitment of additional cells towards this lineage. Counting melanocytes in sections, to rule out excess recruitment towards melanocyte lineage within the crest itself (which would be difficult to detect in whole-mount) revealed that control embryos have the same number of melanocytes in the dorsal neural tube as do ivermectin-treated

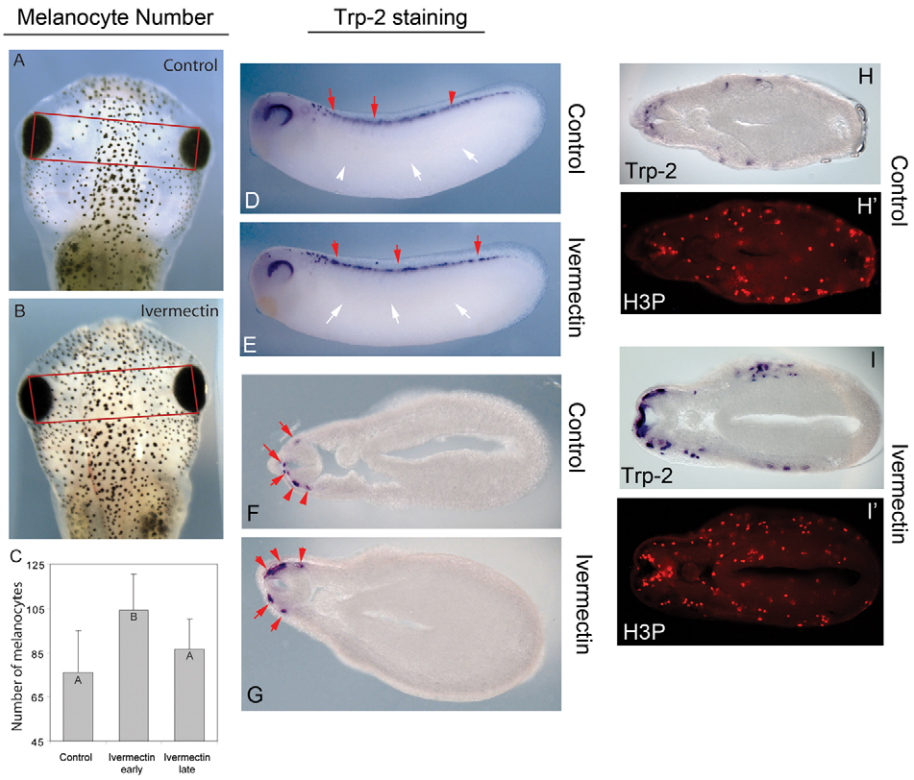

Fig. 3. Early ivermectin exposure induces an increase in pigment cell proliferation. Embryos exposed to ivermectin from stages 10-24 (early) or 28-46 (late) both show darkening due to expansion of melanocytes. To determine whether there was also a corresponding increase in melanocyte number, photographs were taken of controls (A) and ivermectin-exposed (B) embryos after tricaine anesthetization, which contracts the pigment cells. The number of melanocytes in the eye field (red boxes) were then counted. Early exposed embryos showed a 1.5-fold increase in melanocyte number relative to controls (C), whereas no detectable difference was observed between late exposed embryos and controls. Error bars indicate one standard deviation; n=24 embryos for each treatment. Control embryos processed in in situ hybridization for the melanocyte marker *Trp2* at stage 28 show the normal pattern of expression prior to the migration of melanocytes away from the dorsal neural tube (D). Ivermectin-treated embryos show precisely the same pattern (E) and exhibit no evidence of ectopic locations being converted into a melanocyte fate by the ivermectin treatment. Sectioning reveals that control (F) and ivermectin-treated (G) embryos have the same number of melanocytes at the neural tube, also ruling out local shifts of neural crest cells into the melanocyte lineage as the explanation for later hyperpigmentation. Red arrows indicate positive signal (melanocytes indicated by *Trp2* expression), whereas white arrows indicate lack of signal. (H-I′) To directly analyze proliferation in melanocytes, embryos were stained for the melanocyte marker Trp2 using in situ hybridization to identify pigment cells, and were then sectioned and processed for immunohistochemistry with anti-H3B-*P* antibody. (H) Trp2 section in control embryos; (H′) corresponding signal of H3B-*P* stain in the same section. (I) Trp2 section in ivermectin-exposed embryos; (I′) corresponding signal of H3B-*P* stain in the same section. Overlays of the bright-field and fluorescent signals from the same section allowed quantification of the number of melanocytes that were in mitosis. At stage 28, there was no difference (P>0.2, n=6) between controls and ivermectin-treated embryos. By stage 35, there was a significant increase in the number of mitotic melanocytes in the ivermectin-treated embryos (P<0.009, n=6).

embryos (n=10 embryos, P=0.33) (Fig. 3F,G). Given the lack of evidence for recruitment of additional cells into melanocytes at the time when a subset of neural crest cells are assigned a pigment cell fate, we suggest that ivermectin treatment during early stages results in excess melanocytes in later embryos via increased proliferation of mature melanocytes. To confirm the effect on proliferation of melanocytes, we characterized cell proliferation using an antibody to phosphorylated histone 3B (H3B-*P*) – a standard marker of cells in the G2-M transition of the cell cycle, useful for identifying mitotic cells in *Xenopus* (Saka and Smith, 2001; Sanchez Alvarado, 2003). Embryos were stained for the melanocyte marker Trp2 using in situ hybridization to identify melanocytes and then sectioned and processed for immunohistochemistry with anti-H3B-*P* antibody. Overlays of the bright-field (Fig. 3H,H′) and fluorescent (Fig. 3I,I′) signals allowed counting of all melanocytes that were actively dividing (cells positive for both markers). The data are summarized in Table 1, and show that, although embryos exposed at stage 16 and analyzed at stage 28 have the same number of mitotic melanocytes as controls, ivermectin-exposed embryos analyzed at stage 35 have a 2.8-fold increase in the number of melanocytes in mitosis over controls. These data confirm the induction of mitosis in mature melanocytes by ivermectin exposure.

Interestingly, embryos whose ivermectin exposure did not begin until stage 28 (lasting tailbud through tadpole), after a subset of the neural crest has been determined into melanocytes (Kumasaka et al., 2004), did not show a significant increase in melanocytes at stage 46 compared with control animals (Fig. 3C). These results demonstrate that, whereas early-exposed neural crest cells respond to ivermectin by increasing proliferation of committed melanocytes, exposure to ivermectin late in development induces a shape change and aberrant migration in pigment cells but not an increase in proliferation of the melanocytes.

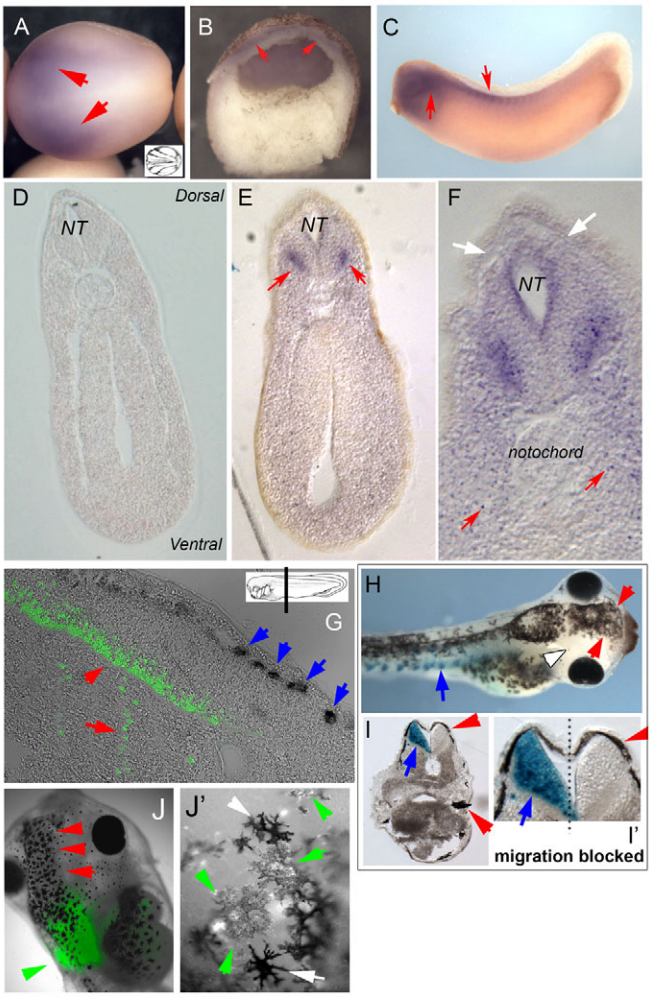

Fig. 4. Expression of GlyCl-α mRNA and protein. In situ hybridization was performed on *Xenopus* embryos with an antisense probe to GlyCl-α. Expression (red arrows) was first detected during neurulation in the developing neural plate (A; panel B shows a thick section in profile because expression was too weak to be clearly visible in thin sections). Expression became restricted during somite stages (C) with foci of staining observed in the ventral marginal zone of the neural tube (NT) (E). Sections also revealed punctate signal in the lateral mesoderm (F, red arrows), which was not observed in the no-primary control (D), and an absence of signal in the dorsal neural tube, where many melanocytes are located (F, white arrows). In panels A-F, red arrows indicate expression of *GlyCl* mRNA, whereas white arrows indicate lack of expression in the dorsal neural tube from which melanocytes originate. Immunohistochemistry (with an antibody to GlyCl; green signal and red arrowheads) and in situ hybridization (with a probe to the melanocyte marker *Trp2*, blue arrows) on the same section of stage-31 embryos (G) revealed that the cells expressing GlyCl are at some distance from melanocytes (melanocytes do not themselves express the ivermectin target protein). (H) As an additional test of long-range signaling, embryos were injected with KCNE1+β-gal mRNA at the 16-cell stage in blastomeres, which resulted in depolarizing potassium channel subunit expression in posterior ventral tissues (blue arrow indicates β-galactosidase lineage label). Red arrowheads in panels H,I indicate hyperpigmentation (aberrant melanocytes) in the region; white arrowhead in H indicates absence of β-gal signal from anterior regions. They were continuously treated with NSC-84093 to prevent melanocyte migration from distant regions of the embryo. Sectioning (I,I') revealed that hyperpigmentation occurred in the head and on the contralateral side, demonstrating that the metastasis-inducing signal is able to cross considerable distance along the anterior-posterior axis (from somites over the gut into the space anterior to the eyes) and across the embryonic midline (red arrowhead in I') even when melanocytes local to the KCNE1 depolarization are prevented from moving. Insets in A and G taken from Nieuwkoop and Faber (Nieuwkoop and Faber, 1967); schematic inset in G shows plane of sections for panels D-G. (J) A small section of neural plate from a ubiquitous GFP-transgenic donor treated with ivermectin (green arrowheads) was transplanted into an untreated host at stage 18, resulting in a hyperpigmentation phenotype (red arrowheads). (J') Similar transplant performed from an ivermectin-treated donor results in GFP-labeled melanocytes (lighter in color owing to overlap of fluorescence and black pigment; green arrowheads) shows that these melanocytes take up ectopic positions next to native melanocytes (white arrowheads) and acquire the same highly arborized shape.

The hyperpigmentation induced by ivermectin is mediated by GlyCl

Having characterized the basic properties of the phenotype, we then investigated the detailed mechanism of action. First, to confirm that the hyperpigmentation effect in *Xenopus* embryos is indeed mediated by GlyCl, and not some off-target property of ivermectin, we exposed embryos to the endogenous ligand of GlyCl, glycine. This control has an additional advantage in that glycine binds to GlyCl at a site different than that used by ivermectin (Shan et al., 2001). Treatment with 0.13 mM glycine induced the same hyperpigmented phenotype as ivermectin (supplementary material Fig. S2), indicating that the modulation of pigment cell number, shape and location by ivermectin is indeed mediated by its effects on GlyCl in *Xenopus*. The same result was obtained by misexpression of a constitutively open mutant GlyCl channel (Beckstead et al., 2002), or by raising endogenous glycine levels by inhibiting the glycine transporter (data not shown).

To identify the embryonic source of the signals induced by ivermectin, we investigated which cells expressed the ivermectin target GlyCl (a ligand-gated chloride channel consisting of a primary α subunit, sufficient for conductance, and a regulator β subunit) (Lynch, 2009). In situ hybridization with an antisense probe for *GlyCl-α1* [homologous to the mammalian glycine receptor subunit α-3 gene (*GLRA3*)] revealed expression in early embryos (Fig. 4A,B) across the neural plate region in a classic horseshoe like pattern indicative of neural crest (Kuriyama and Mayor, 2008). By stage 30, expression was restricted within the anterior central nervous system (Fig. 4C). Sectioning revealed an enriched region in the ventral marginal zone of the neural tube (Fig. 4E, red arrows, compare to sense probe control in Fig. 4D). Higher resolution analysis revealed a punctate stain indicative of a sparse, broadly-distributed cell population (Fig. 4F, red arrows), but no expression in the dorsal neural tube, where melanocyte precursors are located at this stage (Fig. 4G). We conclude that the ivermectin target GlyCl is expressed in embryos, first in a neural-crest-associated pattern and later in a sparse punctate pattern throughout the embryo that is specifically absent from the neural crest cells themselves.

Having determined that the melanocytes themselves are not the cells expressing GlyCl (and thus are not directly depolarized by

Table 1. Proliferation rates in melanocytes

	Number of cells positive for			
Sample	**Trp2**	**H3B-*P***	**Both**	**% Trp2 + H3B-*P***
Stage 35 controls				
1	16	94	3	18.75
2	9	48	1	11.11
3	3	38	0	0.00
4	19	64	0	0.00
5	7	41	1	14.29
			Average	8.83
			S.d.	8.5
Stage 35 ivermectin-exposed				
1	23	102	5	21.74
2	14	115	3	21.43
3	28	102	10	35.71
4	18	63	4	22.22
			Average	25.28
			S.d.	6.97
Stage 28 controls				
1	7	33	0	0.00
2	10	45	2	20.00
3	5	28	4	80.00
4	4	27	2	50.00
			Average	37.50
			S.d.	35.00
Stage 28 ivermectin-exposed				
1	4	33	0	0.00
2	8	35	4	50.00
3	6	32	2	33.33
4	10	30	0	0.00
5	2	27	1	50.00
6	10	28	2	20.00
7	4	28	1	25.00
8	5	30	2	40.00
			Average	27.29
			S.d.	19.92

Embryos were stained with the melanocyte marker Trp2 using in situ hybridization to identify pigment cells and then sectioned and processed for immunohistochemistry with anti-H3B-*P* antibody to identify mitotic cells. Overlays of the images from the same section allowed identification of cells positive for both markers (mitotic melanocytes). Student's *t*-test analysis of the raw data indicates that, although the difference between controls and ivermectin-exposed embryos (8.83% to 25.28%, respectively) at stage 35 is significant (P=0.008), the difference between controls and ivermectin-exposed embryos at stage 28 is not (P=0.233).

ivermectin or glycine), we further tested the apparent cell-non-autonomy of this effect. One cell of embryos at the 32-cell stage was microinjected with mRNA encoding the depolarizing channel subunit KCNE1 (Morokuma et al., 2008) plus mRNA encoding β-galactosidase as a lineage tracer. These embryos were then treated with the MMP-blocking compound NSC-84093, which prevents melanocytes from migrating (Fig. 1D). Embryos in which KCNE1 was injected in a blastomere giving rise to only posterior tissues (Fig. 4H, blue arrow) still exhibited hyperpigmentation (Fig. 4H, white arrowhead). Indeed, analysis of lineage label in sections (Fig. 4I,I′) showed that targeting depolarizing reagents to posterior cells on one side induces the appearance of ectopic, highly dendritic, melanocytes in the head and on the opposite side. Because the migration blocker rules out cell motility as an explanation for the appearance of ectopic melanocytes in the head, we conclude that depolarized cells can exert their inductive effect at long range, not only crossing the midline to affect the contralateral side but signaling at least as far as the length of the head along the anterior-posterior axis. The same conclusion is confirmed by transplantation experiments: small domains of cells from an ivermectin-depolarized donor transplanted into an untreated embryo induce host melanocytes to arborize and migrate inappropriately (Fig. 4J), whereas melanocytes from an ivermectin-depolarized donor migrate to ectopic locations in the host and acquire the same highly dendritic shape (Fig. 4J′).

Hyperpigmentation is mediated by V_{mem} change

To determine whether the alteration of melanocyte behavior was due to GlyCl-dependent changes in transmembrane potential or some other effect of alterations in GlyCl function, we took three approaches: reversing the direction of Cl^- ion flow, depolarization by a GlyCl-independent method and rescue of phenotype by microinjection of a hyperpolarizing channel mRNA.

The intracellular concentration of chloride in frog embryos can be as high as 60 mM, whereas the extracellular concentration in normal 0.1× MMR medium is 10 mM (Gillespie, 1983). To cause hyperpolarization by influx of extracellular chloride into cells via ivermectin-opened GlyCl channels (supplementary material Fig. S1E), we raised the concentration of chloride in the extracellular MMR to 30 mM, 60 mM or 90 mM and examined the resulting phenotype following ivermectin exposure. Elemental analysis comparing control embryos with those reared in ivermectin plus 60 mM chloride showed a 40% increase in chloride by dry weight (0.130% and 0.185%, respectively), demonstrating that external chloride was indeed being taken up by embryonic cells when chloride channels were forced open in high-Cl^- medium.

Raising extracellular chloride levels to 30 mM did not inhibit hyperpigmentation, whereas 60 mM suppressed and 90 mM completely inhibited the phenotype (Table 2). The chloride levels tested had no observable effects on tadpole development beyond inhibiting the hyperpigmenting effects of ivermectin, and these data are precisely the outcome predicted by the Goldman-Katz equation of membrane potential: when the extracellular chloride concentration becomes equal to the intracellular, opening the GlyCl channel with ivermectin no longer depolarizes (no Cl^- ions will leave cells), abolishing the hyperpigmentation phenotype.

If hyperpigmentation is truly a result of membrane depolarization, then cellular voltage modulators that function independently of chloride channels should result in the same phenotype. We therefore tested the effect of disrupting the H^+-V-ATPase hyperpolarizing pump, which we previously showed plays an important role in several voltage-regulated events in *Xenopus* development (Adams et al., 2007; Adams et al., 2006) and controls cellular V_{mem} through movement of H^+, not Cl^-, ions. Injection of low levels of mRNA encoding a well-characterized dominant-negative mutant of Ductin (the 16-kDa proteolipid subunit c of the hyperpolarizing V-ATPase pump complex) into one-cell embryos

Table 2. Using Cl^- levels to modulate voltage-dependent hyperpigmentation

	10 mM Cl^-	30 mM Cl^-	60 mM Cl^-	90 mM Cl^-
Normal pigmentation	0	1	18	32
Hyperpigmented	25	23	5	0
% hyperpigmented	100	95.8	21.7	0
n	25	24	23	32

The number of embryos with each pigmentation phenotype is shown. Embryos were exposed to the chloride channel activator ivermectin (1 μM) from stage 10 through stage 46 in 0.1× MMR containing varying levels of chloride. With the two lowest levels, 10 mM and 30 mM, at which depolarization occurs by exit of chloride ions down their concentration gradient, exposure to ivermectin resulted in strong hyperpigmentation, with nearly all of the exposed embryos developing hyperpigmentation. Exposure to 60 mM chloride, a concentration at which the loss of negative charges from cells is largely diminished, resulted in partial inhibition of hyperpigmentation, and 90 mM, which hyperpolarizes membranes owing to the influx of Cl^-, led to complete inhibition. Embryos raised in the various chloride treatments in the absence of ivermectin showed no abnormal development at the conclusion of the experiment.

resulted in broad, long-lasting (tracked by fused YFP; data not shown) expression, which induced hyperpigmentation in 11.5% of embryos, significantly higher than background hyperpigmentation observed in controls (binomial calculation; n=189 for controls, n=192 for DN-Ductin, P≤0.001) (Fig. 5A-C). Moreover, dn-xDuct-injected hyperpigmented embryos had 2.1-fold more melanocytes than control animals at stage 46 (Student's t-test, t=7.37, n=11 per treatment, P≤0.001; Fig. 5D).

Finally, to confirm that misregulation of melanocyte behavior is induced by depolarization, we performed a rescue experiment. We injected Kir4.1 (Aw et al., 2008), a hyperpolarizing potassium channel (Higashimori and Sontheimer, 2007; Kucheryavykh et al., 2007), into one- or two-cell embryos before placing them into ivermectin. Ivermectin alone induced hyperpigmentation in 97.6% of embryos (n=73), whereas only 73.4% of embryos injected with Kir4.1 were hyperpigmented (n=74), a 25% reduction (Fig. 5E-G). The effect was not cell-autonomous, because Kir4.1 injections into only half of the embryo (one blastomere at the two-cell stage) inhibited hyperpigmentation on both sides of the embryo (Fig. 5H). Together, these data demonstrate that hyperproliferation is induced by depolarization – not by chloride per se or by channel-independent functions of ivermectin or of GlyCl. These results also demonstrate that control of extracellular chloride, together with ivermectin, is a simple and effective technique for rational modulation of transmembrane potential in vivo.

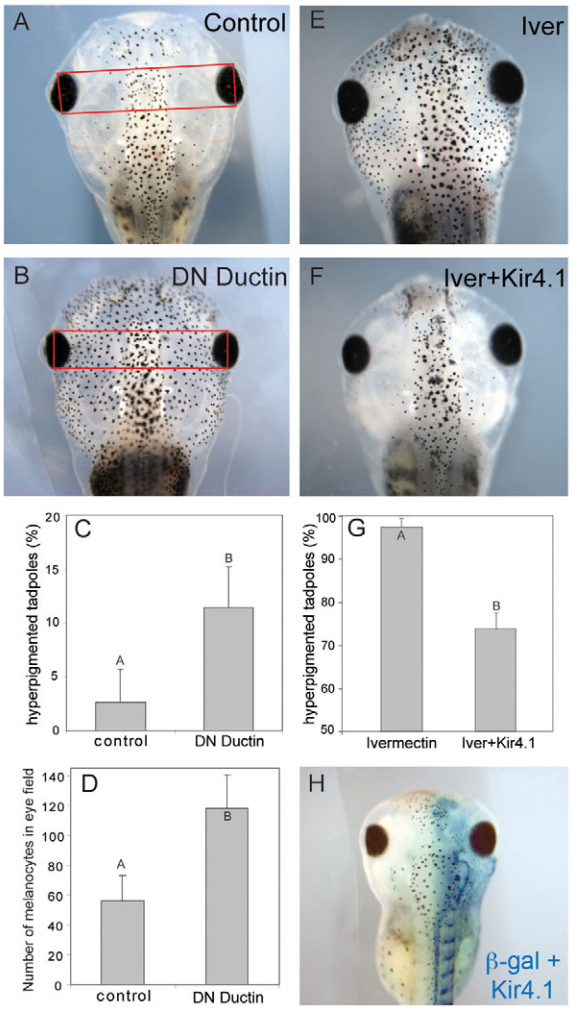

Fig. 5. Hyperpigmentation is due to depolarization. Microinjection of a dominant-negative form of ductin (dn-xDuct) at the one-cell stage inhibits the hyperpolarizing H^+-V-ATPase and results in hyperpigmentation (A,B). Injections result in hyperpigmented tadpoles in 11.5% of embryos (C), significantly higher than background levels observed in control embryos. Hyperpigmented embryos arising from dn-xDuct injections were photographed and the number of melanocytes in the eye field counted; there was a 2.1-fold increase in number of melanocytes compared with age-matched controls (D). By contrast, overexpression of the hyperpolarizing potassium channel Kir4.1 (E,F) inhibits ivermectin-induced hyperpigmentation in 25% of injected embryos (G). Kir4.1-mediated inhibition was non-cell-autonomous, because one of two cell injections, resulting in hyperpolarizing channel activity on just one side of the embryo, inhibited hyperpigmentation on both the left and right side of the embryos (H).

Ivermectin-induced changes in V_{mem} are transduced by serotonin

How do cells sense long-term depolarization and convert this biophysical signal to changes in transcription and cell behavior? We tested three transduction mechanisms that can function downstream of depolarization: influx of Ca^{2+} through voltage-gated calcium channels (VGCC) (Moran, 1991; Munaron et al., 2004a; Munaron et al., 2004b), control of levels of serotonin by electrical modulation of serotonin transporter function (Adams et al., 2006; Fukumoto et al., 2005a; Fukumoto et al., 2005b; Li et al., 2006) and electrophoretic transport of signaling molecules through gap junctions (Anderson and Woodruff, 2001; Brooks and Woodruff, 2004; Levin et al., 2006; Levin and Mercola, 1998; Zhang and Levin, 2009). Our strategy was to apply inhibitors of each of these pathways together with ivermectin, to determine which mechanism is required for depolarization to be effectively transduced into changes of melanocyte behavior.

Treatment with potent VGCC blockers (0.1 mM cadmium chloride, 0.1 mM verapamil) or with the gap junction blocker lindane (1.7 mM) did not result in any reduction in ivermectin-induced hyperpigmentation (Table 3). However, exposure to a specific inhibitor of the serotonin transporter (10 μM fluoxetine) blocked ivermectin-induced hyperpigmentation in all of the treated

Table 3. Rescue of hyperpigmentation phenotype reveals serotonergic involvement

	Control	Ivermectin	Ivermectin + cadmium chloride	Ivermectin + verapamil	Ivermectin + fluoxetine	Ivermectin + lindane
Normally-pigmented tadpoles	57	3	1	0	38	0
Hyperpigmented tadpoles	0	61	47	52	0	48
% hyperpigmented	0	95.3	97.9	100	0	100
n	57	64	48	52	38	48

Embryos were exposed to 10 µM ivermectin from stage 10 through 46 (from gastrulation to organogenesis). Concurrently, they were exposed to one of four drugs; the calcium channel inhibitors cadmium chloride and verapamil, the selective serotonin reuptake inhibitor fluoxetine, and the gap junction inhibitor lindane. Ivermectin alone resulted in a strong incidence of hyperpigmentation, a phenotype that was absent from control embryos. Exposure to cadmium chloride, verapamil or lindane in the presence of ivermectin did not inhibit hyperpigmentation. However, exposure to fluoxetine completely inhibited ivermectin-induced hyperpigmentation. All drugs were used at doses that did not result in any developmental defects.

embryos, without any apparent effects on overall patterning or embryo health.

To determine whether ivermectin-induced depolarization and the function of the serotonin transporter SERT were taking place in the same cells, we performed immunohistochemistry for both receptors on sections of stage 32 *Xenopus* embryos. SERT protein expression significantly overlapped with that of glycine receptors in cells of the ventral neural tube, suggesting that cells sensitive to ivermectin also respond to fluoxetine (Fig. 6A-C).

Fluoxetine increases the availability of extracellular serotonin by blocking its internalization. To ensure that the hyperpigmentation was indeed due to serotonergic signaling and not some other role of SERT or an off-target effect of fluoxetine, we treated embryos with excess extracellular serotonin. This resulted in a consistent and powerful hyperpigmentation (Fig. 6D,E). Taken together, the data strongly suggest that function of the serotonin transporter SERT is required for the transduction of V_{mem} changes into cell behavior changes observed during hyperpigmentation.

Human epidermal melanocytes respond to changes in membrane potential

Although simple in vitro culture cannot demonstrate the non-cell-autonomous effects observed in the embryo, we investigated whether human epidermal melanocytes showed any phenotypes as a result of membrane depolarization. Ivermectin could not be used to depolarize the membrane because the required culture medium of this cell line has a very high chloride content. Instead, we raised extracellular K^+ levels by addition of potassium gluconate, which also depolarizes cells (reduces the ability of K^+ ions to exit cells through potassium channels). This also has the advantage of testing a voltage role independent of chloride per se.

No measurable differences in cell proliferation were noted between melanocytes cultured in standard vs high-K^+ media (data not shown). However, cells grown in high-K^+ medium demonstrated a striking shape change similar to *Xenopus* melanocytes exposed to ivermectin. Following 2 days of culture in 50 mM potassium-gluconate-supplemented medium, human melanocytes developed a highly arborized morphology, with many cells showing five or more projections (compare Fig. 7A with B). Quantification showed that culturing cells in high-K^+ medium had a significant effect on the number of projections on melanocytes (2-way ANOVA, F_3=18.29, P≤0.001). To verify that melanocytes grown in high-K^+ medium were in fact depolarized, we made use of ratiometric V_{mem} imaging using CC2-DMPE and $DiBAC_4(3)$ dyes to visualize the membrane potential (Fig. 7D,E). Comparison of treatments showed depolarization of treated cells compared with controls (Fig. 7F, t_{22}=3.77, P=0.001). We conclude that some of the novel mechanisms that we observed in *Xenopus* larvae are not restricted to embryogenesis and might be relevant to human adult melanocytes.

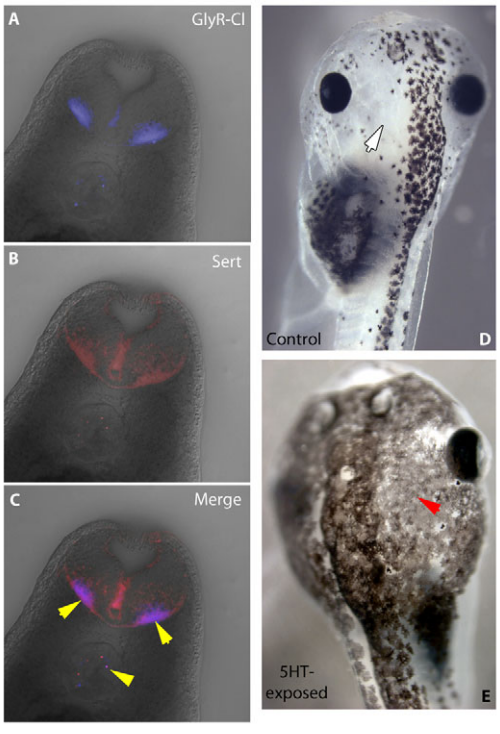

Fig. 6. Serotonergic controls of melanocyte behavior and their relationship to GlyCl-expressing cells. (A) Sections of a stage 32 embryo processed by immunohistochemistry with an anti-GlyCl antibody and visualized with a fluorescent secondary antibody (Alexa Fluor 647). (B) The same section processed by immunohistochemistry with an anti-SERT antibody and visualized with Alexa Fluor 546. (C) Merge of A and B showing colocalization of GlyCl and SERT. Yellow arrowheads indicate areas of overlapping expression (cells containing both GlyCl and SERT). Unlike controls (D), embryos treated with external serotonin acquire the hyperpigmentation phenotype (E), consistent with SERT mediating the effect of depolarized GlyCl-expressing cells on melanocytes. White arrow indicates a region normally devoid of melanocytes; red arrowhead indicates ectopic melanocytes.

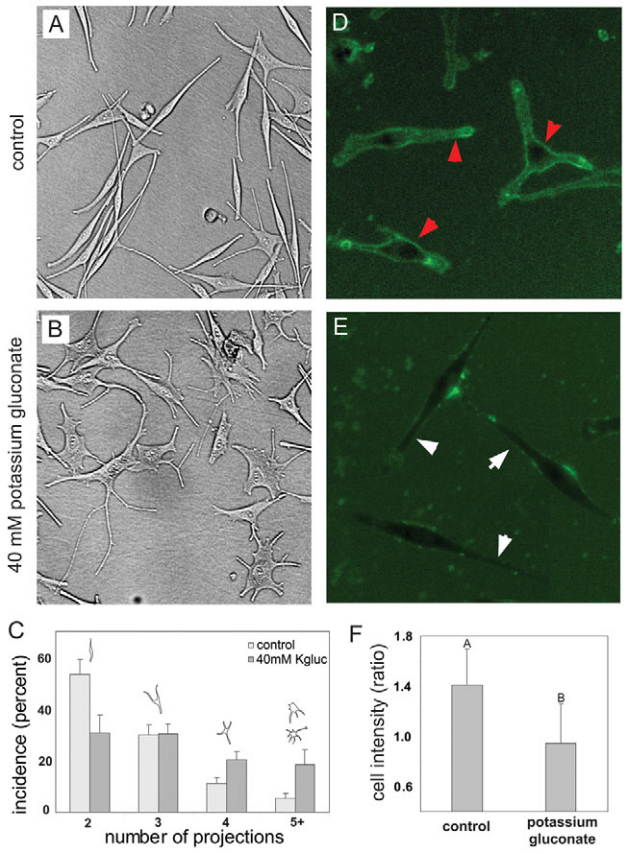

Fig. 7. Human melanocytes exhibit arborization when the membrane is depolarized. In normal culture medium, human melanocytes typically develop two or three projections (A). When grown in media supplemented with 50 mM potassium gluconate, cells develop a more arborized morphology, with many cells having four or five, or more, projections (B). Comparisons between treatments (C) demonstrate a significant effect of potassium gluconate on arborization of melanocytes. Error bars indicate one standard deviation. Image analysis (using the membrane voltage sensor pair CC2-DMPE and $DiBAC_4$) comparing controls (D) and cells cultured in high-potassium medium (E) revealed the predicted depolarization (lower intensity of pixels) in response to the high-potassium media (F). Red arrowheads indicate depolarized cell membranes; white arrows indicate lack of depolarization in membrane.

DISCUSSION

Control of melanocyte behavior by V_{mem}

Prior work has examined the behavior of melanocytes within exogenous electrical fields (Grahn et al., 2003; Stump and Robinson, 1983). However, the role of transmembrane potential in the regulation of neural crest derivatives or the molecular basis for any bioelectrical controls of melanocyte behavior has not previously been examined. Our fundamental finding is that modulation of membrane potential by changing the direction of chloride flux in GlyCl-positive cells robustly and non-cell-autonomously confers a hyperproliferative, inappropriately colonizing phenotype upon melanocytes in *Xenopus* larvae (Fig. 1A-C). Changes in V_{mem} were induced by forcing chloride channels open with the specific agonist ivermectin, followed by control of Cl^- concentration in the medium, a convenient technique with which transmembrane potential can be increased or decreased as desired. The resulting hyperpigmentation in depolarized tadpoles is a result of inappropriate MMP-dependent migration, cell shape change and greater melanocyte number (Fig. 1D; Figs 2, 3); depolarization induced no increase in the amount of melanin pigment per melanocyte. The altered behavior of melanocytes includes arborization, the ability to penetrate and colonize internal organs and neural structures, and the formation of long processes that are highly uncharacteristic of normal melanocytes (Fig. 2). Future work tracing the behavior of small numbers of labeled, depolarized instructor cells transplanted into a wild-type host will be necessary to determine whether the metastasis of ivermectin-treated melanocytes to inappropriate locations is due to altered control of pathfinding at the single-cell level or to a community ('population pressure') effect (Barlow et al., 2008) among high numbers of melanocytes that repel one another (Macmillan, 1976).

There are two phases to the effect. When treatment with depolarizing agent occurs during neurulation, significant increases in pre-melanocyte number occur (a 1.5-fold increase in melanocyte number is observed in periocular skin and a 2.8-fold increase in mitotic melanocytes is observed when all tissues in section are analyzed via H3B-*P* staining). The effect seems to be mediated by increased proliferation of melanocytes, not recruitment of additional cells into the melanocyte lineage (Fig. 3D-G). By contrast, treatment beginning later at organogenesis stages does not induce significant increases in proliferation (Fig. 3C), demonstrating that mitosis and shape and/or migration change in melanocytes are separable processes. Although both changes of melanocyte behavior result from depolarization of transmembrane potential in GlyCl-positive cells, the distinct natures of the two phenotypes is underlined by the fact that, although excess melanocytes do not disappear following withdrawal of ivermectin, shape rapidly returns to normal following washout (Fig. 2G,H).

The early phase might be cell-autonomous, because the chloride channel target is expressed in neural crest cells (precursors of melanocytes) during the time of exposure (Fig. 4A,B). By contrast, the effects of later depolarization are likely to be non-cell-autonomous, because (1) at somite stages the receptor is expressed in cells that are at a considerable distance from the melanocytes whose behavior is altered by induced chloride efflux (Fig. 4F,G), (2) hyperpolarization of cells via Kir4.1 on half of the embryo inhibits hyperpigmentation on both sides (Fig. 5H) and (3) depolarization of posterior cells on one side of the midline results in the appearance of ectopic melanocytes in the head of the embryo on the opposite side even when migration is inhibited (Fig. 4H-I′). Such long-range effects of biophysical changes are a fascinating aspect for future investigation because they suggest opportunities for biomedicine as well as potential sources of unexpected problems in patients taking drugs targeting ion channels.

A connection between ion transport proteins and pigment cell behavior has been observed in zebrafish, specifically between Kir7.1 and melanosomes (Iwashita et al., 2006), as well as between connexin 41.8 and pigment cells (in a diffusion-reaction patterning system) (Asai et al., 1999; Watanabe et al., 2006). However, our data specifically connect the control of V_{mem} in one cell population (GlyCl-expressing instructor cells) with migration, morphology and proliferation in another (pigment cells). Indeed,

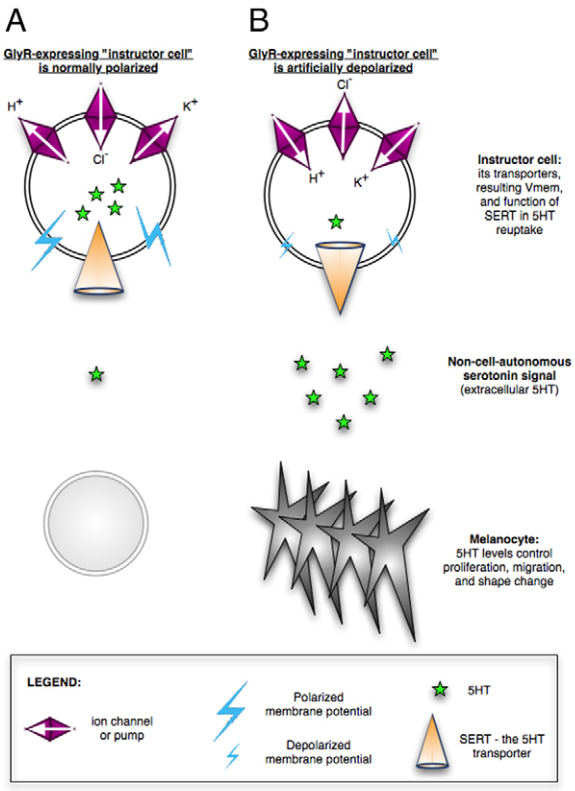

Fig. 8. A model of melanocyte control by transmembrane potential of cells in the neural crest's environment. (A) In unperturbed embryos, several classes of ion transporters keep the plasma membrane polarized. This transmembrane potential powers the reuptake of extracellular serotonin through its transporter SERT, resulting in normal melanocyte behavior. (B) By contrast, when the instructor cell population (demarcated by GlyCl expression) is depolarized by targeted modulation of H^+, Cl^- or K^+ channel/pump function, the SERT runs backwards and not only fails to clear the extracellular space of serotonin, but actually exports additional serotonin. The higher serotonin level in the milieu of the neoblasts induces neoplastic-like behavior in melanocytes, as occurs in human cancers. This pathway can be manipulated at a number of points. Consistent with this model, our data show that, although direct serotonin exposure or depolarization of GlyCl-expressing cells can induce hyperpigmentation, the depolarization phenotype can be prevented by overexpression of hyperpolarizing channels or inhibition of SERT. Central features of this model are the regulation of cell behavior by transmembrane potential, regardless of which specific gene product achieves it, and non-cell-autonomous effects of a cell subpopulation specifically instructing, at considerable distance, one derivative of neural crest to undergo the stem-cell-to-neoplastic-cell-like phenotype.

we show that the phenomenon of membrane-voltage-based signaling is even more directly recapitulated in human pigment cells (Fig. 8), suggesting that the previously observed stimulatory effects of bee venom on human melanocytes (Jeon et al., 2007) is due to the ion-channel-targeting properties of its apamin protein component (Seagar et al., 1984). More broadly, the voltage control mechanism might be a plausible candidate for biomedical intervention in the pigmentation disorder vitiligo (Lotti et al., 2008; Whitton et al., 2008), in melanoma (Yamamura et al., 2008a; Yamamura et al., 2008b) and, more broadly, in neurocristopathies (developmental birth defects involving neural crest stem cell derivatives) (Bolande, 1997; De Schepper et al., 2005; Inoue et al., 2007).

GlyCl as a marker of a unique cell population in embryos

One of the advantages of ivermectin-based depolarization is that the target cells can easily be identified. Ivermectin is a highly specific agonist for GlyCl (Shan et al., 2001), and our phenotype results from the effects on GlyCl rather than off-target side effects of this compound, because its native ligand, glycine, can induce the same effect (supplementary material Fig. S2). Whereas GlyCl is normally expressed in some neurons (spinal cord, retina) and sperm (Lynch, 2009), we detected a dynamic and highly interesting distribution during frog embryogenesis. It is first expressed in the dorsal neural tube during stage 15 (Fig. 4A,B) and is later enriched in the ventral neural tube (Fig. 4C-F), at the same location from which N-tubulin-positive motor neurons arise (Schlosser et al., 2008). At post-neurula stages (e.g. stage 30), it is also present in a unique pattern throughout the interior of the embryo, in a sparse population of small cells resembling macrophages in size (Tomlinson et al., 2008). It is specifically not expressed in melanocytes (Fig. 4G). Importantly, nearly all ivermectin-treated embryos acquire the hyperpigmented phenotype; by contrast, depolarizing arbitrary (even large) groups of cells by forcing KCNE1 overexpression only affects ~20% of the embryos (Morokuma et al., 2008), underscoring the significance of the native GlyCl-expressing cells.

This speckled arrangement of the ivermectin-sensitive cells is especially useful for research because it facilitates exploration of a highly mosaic depolarization effect, a powerful technique resembling the mosaic analysis that has been capitalized on by the *Drosophila* community and is difficult to achieve with ubiquitous V_{mem}-modulating methods such as ionophores. Inducing chloride efflux in a small population of cells induced a highly specific phenotype in which the behavior of melanocytes was radically affected despite completely normal development of the anterior-posterior axis, major organs and other neural crest derivatives such as branchial arches. It is remarkable that depolarization of a rare cell population is able to induce a very specific but almost 100%-penetrant phenotype in just one cell type during embryogenesis.

Transduction, voltage sensing and melanocyte regulation by serotonin

Chloride influx (induced by activation of GlyCl and demonstrated directly using ion chromatography analysis) induces an increase in melanocyte number. Although chloride channels have been linked to mitotic control (Tang et al., 2008; Tung et al., 2009), the pathway resulting in hyperpigmentation is not restricted to chloride-specific signaling but is rather controlled by V_{mem}. This is indicated by the fact that other methods for depolarizing cells, such as inhibition of hyperpolarizing H^+ pumps (Fig. 5A-D) or potassium channels (Fig. 8) (Morokuma et al., 2008), result in the same phenotype. Moreover, the phenotype can be rescued by misexpression of a hyperpolarizing channel (Fig. 5F-H). Thus, the modulation of melanocyte behavior is not a consequence of some cryptic role of ivermectin, nor of the Cl^- ion, but of V_{mem}. However, chloride channels are a tractable mechanism (endogenously, and experimentally) for controlling V_{mem} in distinct cell groups.

It is known that prolonged depolarization activates proliferation of some cell types (Binggeli and Weinstein, 1986; Cone and Tongier, 1971; Olivotto et al., 1996), as we observed in human melanocytes, although the mechanism is largely unknown. Interestingly, sustained ivermectin treatment in *Xenopus* does not result in generalized runaway hyperproliferation but affects a specific cell type; it remains to be understood why the GlyCl-expressing cells instruct only melanocytes and not other cell types. Depolarization induced approximately one extra cell cycle (Fig. 5D and Fig. 3C), which is a very strong effect because it occurred within about a day of exposure, whereas melanocyte doubling normally takes 8-10 days in *Xenopus* (Fukuzawa and Ide, 1983). Thus, depolarization might not be a generalized and direct inducer of mitosis but rather a signal that can stimulate specific instructor cells to trigger a defined and limited change in cell number of specific other cell populations.

Our data are also consistent with previous observations showing abnormal neural crest migration in embryos exposed to electric fields (Borgens and Metcalf, 1994). Although direct application of fields to complex tissues is a somewhat blunter tool than molecular changes of ion fluxes in defined cells, applied electric fields can depolarize cells, and such a treatment also results in hyperpigmentation (data not shown). Because melanocytes do not migrate directionally in physiological direct current (DC) electric fields (Grahn et al., 2003; Isseroff et al., 2001), these effects are probably mediated by transmembrane potential and not long-range electric fields induced by ion channel activity.

How are changes in transmembrane voltage transduced into alterations of cell behavior? Activation of voltage-gated calcium channels is a common mechanism (Nishiyama et al., 2008), although our data (Table 3) offer no support for the role of Ca^{2+} in the depolarization effect. Instead, a serotonin-dependent mechanism is implicated downstream of chloride-dependent V_{mem} changes. Blockade of the serotonin transporter SERT suppresses the hyperpigmentation phenotype (Table 3). Moreover, the well-established role of SERT as part of the reuptake mechanism that lowers extracellular levels of serotonin suggests that high external levels of serotonin ought to mimic the hyperpigmentation effect. This was indeed observed (Fig. 6D,E). The direction of serotonin transport by SERT is controlled by transmembrane potential (Li et al., 2006), and serotonin is a known mitogen (Fanburg and Lee, 1997; Nebigil et al., 2000). Consistently, melanocytes are known to express serotonin receptors (Slominski et al., 2004), and serotonergic signaling has been reported to induce a doubling of melanocytes in human skin (Iyengar, 1998), precisely as we observed.

Together, the data suggest a model in which modulation of serotonin levels (by SERT-dependent clearance of serotonin from intercellular spaces) is a mechanism by which depolarization can activate proliferation. This is particularly plausible for melanocytes because serotonergic signaling has been linked to secretion of α-melanocyte-stimulating hormone (Carr et al., 1991; Slominski et al., 2005); thus, we propose the following model. In unperturbed embryos (Fig. 8A), the 'instructor' cells are polarized by the activity of several ion transporters. The resulting transmembrane gradient powers the function of coexpressed SERT, allowing this reuptake to reduce the level of extracellular serotonin (as occurs in synapses). In the absence of elevated extracellular serotonin levels, melanocytes maintain their normal levels of proliferation, obey normal migration cues and exhibit a rounded shape. By contrast (Fig. 8B), if the membrane is depolarized (by targeting H^+, K^+ or Cl^- transport; Figs 1, 5), SERT cannot clear the surrounding space. Indeed, it runs backwards (Adams and DeFelice, 2002; Hilber et al., 2005) to enrich the milieu with excess serotonin content (Fig. 6D,E). This is a non-cell-autonomous signal and is consistent with a number of serotonin receptors being expressed in melanocytes (Slominski et al., 2005) as well as classical data on serotonergic control of melanocytes in frog skin (van de Veerdonk, 1960).

As in left-right patterning (Fukumoto et al., 2005b; Levin et al., 2006), serotonin acts in this system as a small-molecule messenger mediating cell-cell instructive signaling downstream of changes in transmembrane potential. Indeed, animals injected with serotonin developed neural crest tumors (Nozue and Ono, 1991), suggesting that serotonergic signaling is an important component of tumorigenesis. Future work will identify the receptor mechanisms by which melanocytes respond to serotonin or potential downstream factors to acquire a neoplastic-like phenotype.

Voltage changes in development and cancer

Most cancer cell types exhibit a characteristic depolarization of membrane potential compared with healthy tissue (Blackiston et al., 2009; Kunzelmann, 2005). However, our in vivo experiments revealed a non-cell-autonomous instructive function for GlyCl-expressing cells that would not be apparent from in vitro experiments: depolarization can induce a neoplastic-like phenotype in cells that themselves are not (yet) depolarized (Fig. 4). Strikingly, human melanocytes exhibit an even more direct, cell-autonomous component of the depolarization phenotype (Fig. 7). One of the interesting features of the melanocyte phenotype is the appearance of very long projections (Fig. 2J); it is not yet known whether this is associated with nerves, for example using axons as guidance cues. This might also be related to the striking finding that highly aggressive melanoma cells can be coaxed to produce vascular networks in three-dimensional culture (Maniotis et al., 1999).

Indeed, there is a fascinating and still poorly understood relationship between cancer and developmental processes (Levens, 1990; Rubin, 1985; Waddington, 1935). On transplantation of human metastatic melanoma cells into premigratory neural crest of chick embryos, the melanoma cells became distributed along neural crest migratory pathways, lost tumorigenic potential and acquired normal neural crest features (Fang et al., 2005; Kulesa et al., 2006). Our data illustrate the flip side of normalizing metastatic tumor cells with embryonic microenvironments (Hendrix et al., 2007; Kasemeier-Kulesa et al., 2008; Kulesa et al., 2006): depolarization of somatic cells is a physiological (epigenetic) component of the embryonic microenvironment that, like acidification (Cardone et al., 2005), can contribute to a transformation of the behavior of embryonic stem cell derivatives into cancer-like cells.

Neural crest stem cell derivatives are known to contribute to several tumor types, including melanoma, neuroblastoma and pheochromocytoma (Fuchs and Sommer, 2007). The depolarization phenotype is neoplastic-like – although there is no primary tumor (as in small-cell lung carcinoma, for example), the effect fulfils three classic criteria for cancer: cell shape change, invasiveness and overproliferation. Moreover, the drug NSC-84093 – an MMP

inhibitor (Tomlinson et al., 2009a) – prevents colonization of ectopic sites in the embryo, as it does in adult animal cancer models (Heath and Grochow, 2000). Thus, the hyperpigmentation phenotype seems to be similar in mechanistic ways to the metastatic phase of cancer.

What is the relevance of our data for cancer, and melanoma specifically? Uncontrolled growth and dispersal of melanocytes can lead to melanoma (Kelsh et al., 2000; Stulberg et al., 2003; White and Zon, 2008). Melanoma cell migration (Liu et al., 2004), as well as migration of other cell types (Jin et al., 2003), is known to be dependent on potassium channels (Cruse et al., 2006; Kraft et al., 2003; Liu et al., 2007; Potier et al., 2006; Schwab et al., 1999; Spitzner et al., 2007; Wu et al., 2008) and a number of ion channels have been characterized as markers and likely causes of neoplasm (Arcangeli, 2005; Bennett et al., 2004; Diss et al., 2005; Fraser et al., 2005; Fraser et al., 2000; Lastraioli et al., 2004; Mu et al., 2003; Ouadid-Ahidouch and Ahidouch, 2008; Pardo et al., 1999; Prevarskaya et al., 2007; Wissenbach et al., 2004). Indeed, ion channels are increasingly becoming high-priority targets for anti-neoplastic therapy (Arcangeli et al., 2009; House et al., 2010; Kunzelmann, 2005), and monitoring of electrical properties is being used as a diagnostic tool (Aberg et al., 2005; Dumas and Stoltz, 2005; Gupta et al., 2004; Ouwerkerk et al., 2007). Our data suggest that control of V_{mem} is a key component of this set of pathways, and as such is a promising target of treatments for melanoma as well as other types of neoplasm. In particular, V_{mem} might be an important and novel regulator of the stem cell-cancer cell transition (Kim and Dirks, 2008; Lindvall et al., 2007; Tan et al., 2006; Tataria et al., 2006; Wicha et al., 2006). We are currently pursuing strategies for early, non-invasive cancer detection using voltage-sensitive fluorescent reporter dyes and techniques to normalize cancer by repolarizing neoplastic cells and instructor cell populations.

GlyCl as a target for rational modulation of bioelectric signals in regenerative medicine

It is important to note that the effect described by the above data is not simply a function of the GlyCl protein, nor is it inherently tied to chloride flux (Fig. 5). Although GlyCl is a convenient target for voltage modulation, this pathway is not limited to any one gene product but rather is driven by changes in a biophysical parameter, V_{mem}, that is determined by the activity of multiple transporters. Our data shed light on a control mechanism operating during normal embryogenesis that can regulate neural crest stem cell dynamics, as well as identifying a new environmental parameter that might be involved in neoplastic processes.

Indeed, the data suggest a new strategy for rational control of cell behavior in regenerative medicine. Our method was to identify an ion channel that is present in a specific cell population, and modulate V_{mem} by opening that channel while designing the external medium in such a way as to direct ion flux towards the desired V_{mem} change. We used ivermectin-sensitive GlyCl, which works very well, plus ivermectin is already approved for human use as an antiparasitic (Heukelbach et al., 2004). However, this strategy can be used with any channel (especially potassium channels) for which openers and closers are available, and the above data show that it is possible to use the Goldman-Katz equation to quantitatively design a strategy to rationally modulate transmembrane potential. Previously, we have shown that control of transmembrane potential is a powerful tool for understanding and inducing complex regenerative responses (Adams et al., 2007; Levin, 2007; Levin, 2009a; Sundelacruz et al., 2008). This approach can be used to control V_{mem} changes in well-defined cell groups in vivo with temporal modulation.

Moreover, the unique and unusual expression pattern reveals GlyCl as a marker for a potentially highly important cell type: a kind of 'instructor cell' that can signal other populations (e.g. neural crest) and drastically change their behavior at considerable distance (Fig. 4H-I′, Fig. 5G,H). Analysis of expression of other ion channels and pumps might reveal yet other subsets of otherwise homogenous-seeming cell groups, which, like the GlyCl-expressing cells, could be tractable targets for modulation in regenerative medicine. For example, melanocytes can build vessels through vasculogenic mimicry (Hess et al., 2007; Maniotis et al., 1999), and voltage control should be investigated as a technique for controlling shape in bioengineering contexts (Adams, 2008).

Future work will surely reveal additional fascinating roles for specific ion flows in morphogenesis. Taken together, our data reveal V_{mem} as a tractable mechanism of morphogenetic regulation, with relevance to normal embryonic development and neoplasm, and suggest a pharmacological strategy for V_{mem} modulation that might be of use in several branches of biomedicine.

METHODS

Animal husbandry

Xenopus embryos were maintained according to standard protocols (Sive et al., 2000) in 0.1× MMR, pH 7.8, plus 0.1% gentamicin. *Xenopus* embryos were staged according to Nieuwkoop and Faber (Nieuwkoop and Faber, 1967).

Expression analysis

In situ hybridization was performed as previously described (Harland, 1991). *Xenopus* embryos were collected and fixed in MEMFA (Sive et al., 2000). Prior to in situ hybridization, embryos were washed in phosphate buffered saline (PBS) + 0.1% Tween-20 (PBST) and then transferred to methanol through a 25%/50%/75% series. Probes for in situ hybridization were generated in vitro from linearized templates using a DIG labeling mix from Roche. Chromogenic reaction times optimized signal:background ratio. Analyses represent consistent patterns from 50-60 embryos for each marker. Probes used for in situ hybridization include: sense and antisense GlyCl-α (NCBI accession #CX801861), and GlyCl-β (NCBI accession #BC121237). Anti-GlyCl (Chemicon 5052 used at 1:200 dilution) and -SERT (Chemicon MAB5618 used at 1:100 dilution) antibodies were used for immunohistochemistry using previously described protocols (Levin, 2004).

Microinjection

Capped, synthetic mRNAs were dissolved in water and injected into embryos in 3% Ficoll using standard methods (Sive et al., 2000). After 3 hours, embryos were washed and cultured in 0.1× MMR until the desired stages were reached. Constructs used for misexpression included: dominant-negative E140K mutant of ductin (the 16 kDa subunit of the V-ATPase) (Adams et al., 2006; Finbow et al., 1995), the KCNE1 accessory subunit (Morokuma et al., 2008), the GlyCl wild-type channel (Davies et al., 2003) and the potassium channel Kir4.1 (Aw et al., 2008).

Drug exposure

Stocks of ivermectin (Sigma) were kept at 10 mM concentration in dimethyl sulfoxide (DMSO). Embryos were exposed in 0.1× MMR for the stages indicated to: ivermectin, 1 μM; cadmium chloride, 0.1 mM; verapamil, 10 μM; fluoxetine, 10 μM; lindane, 1.7 mM; NSC-84093, 2 μM; and glycine, 0.13 mM.

Elemental analysis

For elemental analysis, cohorts of stage 13 embryos were either untreated or exposed to a combination of 10 μM ivermectin + MMR containing 60 mM Cl^-. At stage 30, 2 ml of packed embryo were collected from each cohort and washed three times in 0.1× MMR. Excess media was removed from the samples and the embryos were stored at −80°C before shipping to Galbraith Laboratories (Knoxville, TN) for dry analysis of chlorine concentration. Samples were prepared by Parr oxygen bomb combustion and analyzed by ion chromatography. Results are reported as percent chloride in total sample based on dry mass.

Measurement of melanocyte numbers

Melanocytes were counted by cellAnalyst software (AssaySoft) on digital photographs of anesthetized larvae. Adobe Illustrator was used to define the dorsal region between the eyes used for counting. Tail regions were defined using digital photographs: all melanocytes within a 400×400 pixel box, extending anteriorly from the tip of the tail, were counted.

Immunohistochemistry

Spatial detection of apoptosis and proliferation was performed by immunohistochemistry in section. We chose caspase-3 staining as a more specific detector of apoptosis (Chakraborty et al., 2006; Makino et al., 2005; Yu et al., 2002) than classical methods such as TUNEL, which gives considerable levels of false positive signal (Stahelin et al., 1998). Briefly, larvae were fixed overnight in MEMFA (Sive et al., 2000), embedded in agarose and sectioned at 100 μm using a Leica vibratome. The sections were permeabilized in PBS + 0.1% Triton X-100 for 30 minutes, blocked with 10% goat serum PBST for 1 hour, and incubated at 4°C overnight with primary antibody (anti-activated-caspase-3; Abcam #AB13847) for apoptosis (Frankfurt, 1990), or anti-H3B-*P*, Upstate #05-598) for proliferation, diluted 1:1000 in PBST + 10% goat serum. They were then washed six times with PBST (1 hour each at room temperature) and incubated with Alexa-Fluor-555-conjugated secondary antibody at 1:1000 in PBST + 10% goat serum overnight at 4°C. Sections were photographed using the appropriate filter set on a Nikon SMZ-1500 scope with epifluorescence after six 1-hour washes in PBST.

Direct measurement of melanin content

Melanin content of embryos was measured as described previously (Pogge v Strandmann et al., 2000) with slight modification. In brief, five stage-45 embryos were hydrolyzed in 0.2 ml 1 M NaOH for 96 hours at 37°C, and 0.15 ml was diluted to 1 ml with H_2O, and used for spectrophotometric determination of the absorption at 414 nm.

Human melanocyte culture

Human melanocytes were obtained commercially and cultured in DermaLife M Melanocyte culture medium (cells and media provided by Lifeline Cell Technology, Walkersville, MD). Cells were maintained in standard 25-cm^2 culture flasks; the 10 ml of media was replaced every other day. On reaching confluence, melanocytes were passaged using a standard trypsinization protocol, and new colonies were seeded at approximately 5000 cells/cm^2. For high-potassium-media experiments, DermaLife M media was supplemented with 40 mM potassium gluconate, a level determined during a preliminary potassium dose-response screen to be non-inhibitory to growth while inducing morphological changes.

For cell shape analysis, cells were imaged on a Nikon AZ100M stereomicroscope and the numbers of filopodia on all cells within

TRANSLATIONAL IMPACT

Clinical issue

Understanding how stem cells function in the creation and maintenance of biological shape is fundamental to three main areas of biomedicine: birth defects, which result from failure to build appropriate structures during embryonic development; regeneration after injury or disease, which requires the proper shape of the damaged structure to be rebuilt in adulthood; and, finally, cancer, which can be seen as a failure to obey the patterning cues that continuously act to impose three-dimensional order against neoplasia and aging. The neural crest is a key population of stem cells that migrate throughout the embryo and contribute to structures such as the heart, face and skin. Neurocristopathies, which are defects in neural crest development, form an important class of congenital defects.

Although the genetic and biochemical signaling pathways that regulate the conversion from normal developmental patterning to cancer have been intensively studied, an important class of signals remains poorly understood: endogenous bioelectric cues produced by ion channels and transmembrane voltage gradients.

Results

Owing to their ease of manipulation and relative transparency, *Xenopus laevis* embryos are a particularly convenient model for understanding the signals directing neural crest cells and their progeny. To determine how changes in membrane voltage regulate cell behavior and interactions in vivo, the authors target a population of cells expressing the glycine-gated chloride channel (GlyCl). By opening the channel pharmacologically and manipulating ion levels to hyperpolarize or depolarize these cells, they show that GlyCl-expressing cells can trigger a neoplastic-like phenotype in an important class of neural crest derivatives – the pigment cells known as melanocytes. The GlyCl-expressing 'instructor' cells trigger hyperproliferation, and cause increased dendricity and invasiveness into neural tissues, blood vessels and gut. Crucially, the induction of this metastatic phenotype occurs at long range and is mediated by serotonergic signaling.

Implications and future directions

This work demonstrates that the bioelectrical state of specific cells in the host can trigger the stem cell to neoplastic cell transition in pigment cells, resulting in a phenotype that is similar to that of metastatic melanoma. Crucially, the relevant signal is not tied to GlyCl per se, or even chloride, but is truly carried by a physiological parameter – voltage. These data reveal a new role for ion flow and serotonergic signaling in melanocyte regulation, with potential uses in the treatment of vitiligo and melanoma. Furthermore, they uncover a newly identified population of 'instructor' cells (characterized by GlyCl expression) that can control the fate of neural crest derivatives with exquisite specificity. The ability to modulate membrane voltage without the need for gene therapy, and the identification of cell types that can direct the function of stem cells, are powerful approaches through which to better understand and address the in vivo control of patterning in cancer, the regenerative response and the repair of birth defects.

doi:10.1242/dmm.006650

the field of vision were counted. Cell culture in high-potassium media was repeated three times and the results averaged for statistical analysis.

Imaging V_{mem} using CC2-DMPE and $DiBAC_4(3)$

CC2-DMPE [N-(6-chloro-7-hydroxycoumarin-3-carbonyl)-dimyristoylphosphatidyl ethanolamine], a cationic coumarin phospholipid, and the anionic oxonol $DiBAC_4(3)$ [bis-(1,3-dibutylbarbituric acid) trimethine oxonol] were purchased from Invitrogen. Using two dyes with opposite emission profiles simultaneously provides an internal control and allows results to be corrected for artifact by ratiometric normalization. Stock CC2-DMPE solution was prepared according to manufacturer's directions: a 5 mM stock (in DMSO) was prepared, aliquoted and stored at –20°C until immediately before use. $DiBAC_4(3)$ stock (1.9 mM in DMSO) was prepared and stored at room temperature. CC2-DMPE stock was dissolved 1:1000 directly into culture medium. $DiBAC_4(3)$ stock was dissolved 1:2 in DMSO, then spun at RCF 20,800 for 10 minutes to remove undissolved particles of dye. Supernatant was then diluted 1:4000 in culture media. 1 ml of CC2-DMPE was added to cells grown in 35-mm FluoroDish Sterile Culture Dishes. Cells were incubated for 30 minutes, then washed twice with plain culture media. 1-2 ml of $DiBAC_4(3)$ were then added to the dish. Cells were incubated at least 30 minutes before imaging began; cells were imaged while in the $DiBAC_4(3)$ bath. A round coverslip was dropped into the dish, and any medium outside the well was removed. The dish was then turned over and the cells imaged through the glass bottom of the dish.

An Olympus BX-61 equipped with a Hamamatsu ORCA AG CCD camera, and controlled by IPLabs, was used for imaging. CC2-DMPE is imaged with the following filters: EX 405/20; BS 425; EM 460/50 (Chroma filter set 31036). $DiBAC_4(3)$ is imaged with: EX 470/20; BS 485; EM 517/23 (Chroma filter set 41001). After dark-field (to remove camera noise) and flat-field (to correct for uneven illumination) corrections, image arithmetic was used to take the ratio of CC2-DMPE intensity over $DiBAC_4(3)$ intensity. The result is an artifact-corrected picture of V_{mem}; the brighter the pixel, the more polarized the region it represents. Images were pseudocolored to make the contrast between different regions more easily visible. No calibration was performed; nonetheless, pixel intensity within and among images can be compared for relative quantification. Except for resizing during figure preparation, no other changes were made to the images; thus, pixel intensity or color are reliable reporters of V_{mem}. Original images are available on request.

Statistics

All statistical analyses were performed using Prism v.5 (GraphPad Software, La Jolla, CA). Student's *t*-tests were used for comparisons of melanocyte number, incidence of hyperpigmented tadpoles and cell intensity for microscopy experiments. Filopodial numbers in human melanocytes were compared using a two-way ANOVA. Data conformed to parametric requirements; no corrections were needed for normality or variance.

ACKNOWLEDGEMENTS

We thank Punita Koustubhan and Amber Currier for *Xenopus* husbandry, and Dayong Qiu and Norman Lautsch for histology. We are grateful to the Drug Synthesis and Chemistry Branch, Developmental Therapeutics program, Division of Cancer Treatment and Diagnosis, National Cancer Institute, for providing NSC-84093 compound, Daryl Davies and Miriam Fine for the GlyCl expression construct, John Mihic for useful discussions and for the overactive D97R mutant of human glyRα1, Nancy Papalopulu for helpful comments on the manuscript, and Carole Labonne for Sox10 plasmid. M. Levin gratefully acknowledges the support of the NIH (grant GM078484), NHTSA (grant DTNH22-06-G-00001) and DOD (grant W81XWH-10-2-0058). D.B. was supported by Forsyth Institute's T32-DE-007327 training grant. D.S.A. was supported by the NIH/NIDCR (grant K22DE016633).

COMPETING INTERESTS

The authors declare no competing financial interests.

AUTHOR CONTRIBUTIONS

D.B. and M. Levin conceived and carried out the experiments; D.B. and D.S.A. performed voltage dye imaging and analysis; J.M.L. created overexpression DNA constructs; M. Lobikin performed mitotic and apoptotic cell analyses; D.B., M. Levin and D.S.A. wrote the paper.

SUPPLEMENTARY MATERIAL

Supplementary material for this article is available at http://dmm.biologists.org/lookup/suppl/doi:10.1242/dmm.005561/-/DC1

REFERENCES

Aberg, P., Geladi, P., Nicander, I., Hansson, J., Holmgren, U. and Ollmar, S. (2005). Non-invasive and microinvasive electrical impedance spectra of skin cancer-a comparison between two techniques. *Skin Res. Technol.* **11**, 281-286.

Adams, D. S. (2008). A new tool for tissue engineers: ions as regulators of morphogenesis during development and regeneration. *Tissue Eng. Part A* **14**, 1461-1468.

Adams, D. S. and Levin, M. (2006a). Inverse drug screens: a rapid and inexpensive method for implicating molecular targets. *Genesis* **44**, 530-540.

Adams, D. S. and Levin, M. (2006b). Strategies and techniques for investigation of biophysical signals in patterning. In *Analysis of Growth Factor Signaling in Embryos* (ed. M. Whitman and A. K. Sater), pp. 177-262. Taylor and Francis Books.

Adams, D. S., Robinson, K. R., Fukumoto, T., Yuan, S., Albertson, R. C., Yelick, P., Kuo, L., McSweeney, M. and Levin, M. (2006). Early, H^+-V-ATPase-dependent proton flux is necessary for consistent left-right patterning of non-mammalian vertebrates. *Development* **133**, 1657-1671.

Adams, D. S., Masi, A. and Levin, M. (2007). H^+ pump-dependent changes in membrane voltage are an early mechanism necessary and sufficient to induce Xenopus tail regeneration. *Development* **134**, 1323-1335.

Adams, S. V. and DeFelice, L. J. (2002). Flux coupling in the human serotonin transporter. *Biophys. J.* **83**, 3268-3282.

Al-Hajj, M., Becker, M. W., Wicha, M., Weissman, I. and Clarke, M. F. (2004). Therapeutic implications of cancer stem cells. *Curr. Opin. Genet. Dev.* **14**, 43-47.

Anderson, K. L. and Woodruff, R. I. (2001). A gap junctionally transmitted epithelial cell signal regulates endocytic yolk uptake in Oncopeltus fasciatus. *Dev. Biol.* **239**, 68-78.

Arcangeli, A. (2005). Expression and role of hERG channels in cancer cells. *Novartis Found. Symp.* **266**, 225-232; discussion 232-234.

Arcangeli, A., Crociani, O., Lastraioli, E., Masi, A., Pillozzi, S. and Becchetti, A. (2009). Targeting ion channels in cancer: a novel frontier in antineoplastic therapy. *Curr. Med. Chem.* **16**, 66-93.

Asai, R., Taguchi, E., Kume, Y., Saito, M. and Kondo, S. (1999). Zebrafish leopard gene as a component of the putative reaction-diffusion system. *Mech. Dev.* **89**, 87-92.

Aw, S., Adams, D. S., Qiu, D. and Levin, M. (2008). H,K-ATPase protein localization and Kir4.1 function reveal concordance of three axes during early determination of left-right asymmetry. *Mech. Dev.* **125**, 353-372.

Barlow, A. J., Wallace, A. S., Thapar, N. and Burns, A. J. (2008). Critical numbers of neural crest cells are required in the pathways from the neural tube to the foregut to ensure complete enteric nervous system formation. *Development* **135**, 1681-1691.

Baylin, S. B. and Ohm, J. E. (2006). Epigenetic gene silencing in cancer-a mechanism for early oncogenic pathway addiction? *Nat. Rev. Cancer* **6**, 107-116.

Beckstead, M. J., Phelan, R., Trudell, J. R., Bianchini, M. J. and Mihic, S. J. (2002). Anesthetic and ethanol effects on spontaneously opening glycine receptor channels. *J. Neurochem.* **82**, 1343-1351.

Bennett, E. S., Smith, B. A. and Harper, J. M. (2004). Voltage-gated Na^+ channels confer invasive properties on human prostate cancer cells. *Pflugers Arch.* **447**, 908-914.

Bergstrom, C. S., Saunders, R. A., Hutchinson, A. K. and Lambert, S. R. (2005). Iris hypoplasia and aorticopulmonary septal defect: a neurocristopathy. *J. AAPOS* **9**, 264-267.

Biagiotti, T., D'Amico, M., Marzi, I., Di Gennaro, P., Arcangeli, A., Wanke, E. and Olivotto, M. (2006). Cell renewing in neuroblastoma: electrophysiological and immunocytochemical characterization of stem cells and derivatives. *Stem Cells* **24**, 443-453.

Binggeli, R. and Weinstein, R. (1986). Membrane potentials and sodium channels: hypotheses for growth regulation and cancer formation based on changes in sodium channels and gap junctions. *J. Theor. Biol.* **123**, 377-401.
Bissell, M. J. and Labarge, M. A. (2005). Context, tissue plasticity, and cancer: are tumor stem cells also regulated by the microenvironment? *Cancer Cell* **7**, 17-23.
Bjerkvig, R., Tysnes, B. B., Aboody, K. S., Najbauer, J. and Terzis, A. J. (2005). Opinion: the origin of the cancer stem cell: current controversies and new insights. *Nat. Rev. Cancer* **5**, 899-904.
Blackiston, D. J., McLaughlin, K. A. and Levin, M. (2009). Bioelectric controls of cell proliferation: ion channels, membrane voltage and the cell cycle. *Cell Cycle* **8**, 3519-3528.
Bolande, R. P. (1997). Neurocristopathy: its growth and development in 20 years. *Pediatr. Pathol. Lab. Med.* **17**, 1-25.
Borgens, R. and Metcalf, M. (1994). Weak applied voltages interfere with amphibian morphogenesis and pattern. *J. Exp. Zool.* **268**, 323-338.
Borgens, R., Robinson, K., Vanable, J. and McGinnis, M. (1989). *Electric Fields in Vertebrate Repair.* New York: Alan R. Liss.
Brooks, R. A. and Woodruff, R. I. (2004). Calmodulin transmitted through gap junctions stimulates endocytic incorporation of yolk precursors in insect oocytes. *Dev. Biol.* **271**, 339-349.
Bulic-Jakus, F., Ulamec, M., Vlahovic, M., Sincic, N., Katusic, A., Juric-Lekc, G., Serman, L., Kruslin, B. and Belicza, M. (2006). Of mice and men: teratomas and teratocarcinomas. *Coll. Antropol.* **30**, 921-924.
Cai, J., Cheng, A., Luo, Y., Lu, C., Mattson, M. P., Rao, M. S. and Furukawa, K. (2004). Membrane properties of rat embryonic multipotent neural stem cells. *J. Neurochem.* **88**, 212-226.
Cardone, R. A., Casavola, V. and Reshkin, S. J. (2005). The role of disturbed pH dynamics and the Na+/H+ exchanger in metastasis. *Nat. Rev. Cancer* **5**, 786-795.
Carr, J. A., Saland, L. C., Samora, A., Benavidez, S. and Krobert, K. (1991). In vivo effects of serotonergic agents on alpha-melanocyte-stimulating hormone secretion. *Neuroendocrinology* **54**, 616-622.
Chakraborty, C., Nandi, S. S., Sinha, S. and Gera, V. K. (2006). Zebrafish caspase-3: molecular cloning, characterization, crystallization and phylogenetic analysis. *Protein Pept. Lett.* **13**, 633-640.
Cho, T., Bae, J. H., Choi, H. B., Kim, S. S., McLarnon, J. G., Suh-Kim, H., Kim, S. U. and Min, C. K. (2002). Human neural stem cells: electrophysiological properties of voltage-gated ion channels. *NeuroReport* **13**, 1447-1452.
Collazo, A., Bronner-Fraser, M. and Fraser, S. E. (1993). Vital dye labelling of Xenopus laevis trunk neural crest reveals multipotency and novel pathways of migration. *Development* **118**, 363-376.
Cone, C. D. and Cone, C. M. (1976). Induction of mitosis in mature neurons in central nervous system by sustained depolarization. *Science* **192**, 155-158.
Cone, C. D. and Tongier, M. (1971). Control of somatic cell mitosis by simulated changes in the transmembrane potential level. *Oncology* **25**, 168-182.
Cooper, C. D. and Raible, D. W. (2009). Mechanisms for reaching the differentiated state: Insights from neural crest-derived melanocytes. *Semin. Cell Dev. Biol.* **20**, 105-110.
Crane, J. F. and Trainor, P. A. (2006). Neural crest stem and progenitor cells. *Annu. Rev. Cell Dev. Biol.* **22**, 267-286.
Cruse, G., Duffy, S. M., Brightling, C. E. and Bradding, P. (2006). Functional KCa3.1 K+ channels are required for human lung mast cell migration. *Thorax* **61**, 880-885.
Davies, D. L., Trudell, J. R., Mihic, S. J., Crawford, D. K. and Alkana, R. L. (2003). Ethanol potentiation of glycine receptors expressed in Xenopus oocytes antagonized by increased atmospheric pressure. *Alcohol. Clin. Exp. Res.* **27**, 743-755.
De Schepper, S., Boucneau, J., Lambert, J., Messiaen, L. and Naeyaert, J. M. (2005). Pigment cell-related manifestations in neurofibromatosis type **1**, an overview. *Pigment Cell Res.* **18**, 13-24.
Diss, J. K., Stewart, D., Pani, F., Foster, C. S., Walker, M. M., Patel, A. and Djamgoz, M. B. (2005). A potential novel marker for human prostate cancer: voltage-gated sodium channel expression in vivo. *Prostate Cancer Prostatic Dis.* **8**, 266-273.
Domen, J. and Weissman, I. L. (2000). Hematopoietic stem cells need two signals to prevent apoptosis; BCL-2 can provide one of these, Kitl/c-Kit signaling the other. *J. Exp. Med.* **192**, 1707-1718.
Domen, J., Gandy, K. L. and Weissman, I. L. (1998). Systemic overexpression of BCL-2 in the hematopoietic system protects transgenic mice from the consequences of lethal irradiation. *Blood* **91**, 2272-2282.
Ducasse, M. and Brown, M. A. (2006). Epigenetic aberrations and cancer. *Mol. Cancer* **5**, 60.
Dumas, D. and Stoltz, J. F. (2005). New tool to monitor membrane potential by FRET Voltage Sensitive Dye (FRET-VSD) using Spectral and Fluorescence Lifetime Imaging Microscopy (FLIM). Interest in cell engineering. *Clin. Hemorheol. Microcirc.* **33**, 293-302.
Fanburg, B. and Lee, S. (1997). A new role for an old molecule: serotonin as a mitogen. *Am. J. Physiol.* **272**, L795-L806.
Fang, D., Nguyen, T. K., Leishear, K., Finko, R., Kulp, A. N., Hotz, S., Van Belle, P. A., Xu, X., Elder, D. E. and Herlyn, M. (2005). A tumorigenic subpopulation with stem cell properties in melanomas. *Cancer Res.* **65**, 9328-9337.
Finbow, M. E., Harrison, M. and Jones, P. (1995). Ductin-a proton pump component, a gap junction channel and a neurotransmitter release channel. *BioEssays* **17**, 247-255.
Frankfurt, O. S. (1990). Decreased stability of DNA in cells treated with alkylating agents. *Exp. Cell Res.* **191**, 181-185.
Fraser, S. P., Grimes, J. A. and Djamgoz, M. B. (2000). Effects of voltage-gated ion channel modulators on rat prostatic cancer cell proliferation: comparison of strongly and weakly metastatic cell lines. *Prostate* **44**, 61-76.
Fraser, S. P., Diss, J. K., Chioni, A. M., Mycielska, M. E., Pan, H., Yamaci, R. F., Pani, F., Siwy, Z., Krasowska, M., Grzywna, Z. et al. (2005). Voltage-gated sodium channel expression and potentiation of human breast cancer metastasis. *Clin. Cancer Res.* **11**, 5381-5389.
Fuchs, S. and Sommer, L. (2007). The neural crest: understanding stem cell function in development and disease. *Neurodegen. Dis.* **4**, 6-12.
Fukumoto, T., Blakely, R. and Levin, M. (2005a). Serotonin transporter function is an early step in left-right patterning in chick and frog embryos. *Dev. Neurosci.* **27**, 349-363.
Fukumoto, T., Kema, I. P. and Levin, M. (2005b). Serotonin signaling is a very early step in patterning of the left-right axis in chick and frog embryos. *Curr. Biol.* **15**, 794-803.
Fukuzawa, T. and Ide, H. (1983). Proliferation in vitro of melanophores from Xenopus laevis. *J. Exp. Zool.* **226**, 239-244.
Gersdorff Korsgaard, M. P., Christophersen, P., Ahring, P. K. and Olesen, S. P. (2001). Identification of a novel voltage-gated Na+ channel rNa(v)1.5a in the rat hippocampal progenitor stem cell line HiB5. *Pflugers Arch.* **443**, 18-30.
Gillespie, J. I. (1983). The distribution of small ions during the early development of Xenopus laevis and Ambystoma mexicanum embryos. *J. Physiol.* **344**, 359-377.
Gonzalez, C. (2007). Spindle orientation, asymmetric division and tumour suppression in Drosophila stem cells. *Nat. Rev. Genet.* **8**, 462-472.
Grahn, J. C., Reilly, D. A., Nuccitelli, R. L. and Isseroff, R. R. (2003). Melanocytes do not migrate directionally in physiological DC electric fields. *Wound Repair Regen.* **11**, 64-70.
Gupta, D., Lis, C. G., Dahlk, S. L., Vashi, P. G., Grutsch, J. F. and Lammersfeld, C. A. (2004). Bioelectrical impedance phase angle as a prognostic indicator in advanced pancreatic cancer. *Br. J. Nutr.* **92**, 957-962.
Haass, N. K. and Herlyn, M. (2005). Normal human melanocyte homeostasis as a paradigm for understanding melanoma. *J. Investig. Dermatol. Symp. Proc.* **10**, 153-163.
Haass, N. K., Smalley, K. S., Li, L. and Herlyn, M. (2005). Adhesion, migration and communication in melanocytes and melanoma. *Pigment Cell Res.* **18**, 150-159.
Harland, R. (1991). In situ hybridization: an improved whole mount method for *Xenopus* embryos. In *Xenopus laevis: Practical Uses in Cell and Molecular Biology*, Vol. 36 (ed. B. Kay and H. Peng), pp. 685-695. San Diego: Academic Press.
Heath, E. I. and Grochow, L. B. (2000). Clinical potential of matrix metalloprotease inhibitors in cancer therapy. *Drugs* **59**, 1043-1055.
Hendrix, M. J., Seftor, E. A., Seftor, R. E., Kasemeier-Kulesa, J., Kulesa, P. M. and Postovit, L. M. (2007). Reprogramming metastatic tumour cells with embryonic microenvironments. *Nat. Rev. Cancer* **7**, 246-255.
Hess, A. R., Margaryan, N. V., Seftor, E. A. and Hendrix, M. J. (2007). Deciphering the signaling events that promote melanoma tumor cell vasculogenic mimicry and their link to embryonic vasculogenesis: role of the Eph receptors. *Dev. Dyn.* **236**, 3283-3296.
Heubach, J. F., Graf, E. M., Leutheuser, J., Bock, M., Balana, B., Zahanich, I., Christ, T., Boxberger, S., Wettwer, E. and Ravens, U. (2004). Electrophysiological properties of human mesenchymal stem cells. *J. Physiol.* **554**, 659-672.
Heukelbach, J., Winter, B., Wilcke, T., Muehlen, M., Albrecht, S., de Oliveira, F. A., Kerr-Pontes, L. R., Liesenfeld, O. and Feldmeier, H. (2004). Selective mass treatment with ivermectin to control intestinal helminthiases and parasitic skin diseases in a severely affected population. *Bull. World Health Organ.* **82**, 563-571.
Higashimori, H. and Sontheimer, H. (2007). Role of Kir4.1 channels in growth control of glia. *GLIA* **55**, 1668-1679.
Hilber, B., Scholze, P., Dorostkar, M. M., Sandtner, W., Holy, M., Boehm, S., Singer, E. A. and Sitte, H. H. (2005). Serotonin-transporter mediated efflux: a pharmacological analysis of amphetamines and non-amphetamines. *Neuropharmacology* **49**, 811-819.
Hong, D., Gupta, R., Ancliff, P., Atzberger, A., Brown, J., Soneji, S., Green, J., Colman, S., Piacibello, W., Buckle, V. et al. (2008). Initiating and cancer-propagating cells in TEL-AML1-associated childhood leukemia. *Science* **319**, 336-339.
House, C. D., Vaske, C. J., Schwartz, A., Obias, V., Frank, B., Luu, T., Sarvazyan, N., Irby, R. B., Strausberg, R. L., Hales, T. et al. (2010). Voltage-gated Na^+ channel SCN5A is a key regulator of a gene transcriptional network that controls colon cancer invasion. *Cancer Res.* **70**, 6957-6967.
Ingber, D. E. (2008). Can cancer be reversed by engineering the tumor microenvironment? *Semin. Cancer Biol.* **18**, 356-364.
Ingber, D. E. and Levin, M. (2007). What lies at the interface of regenerative medicine and developmental biology? *Development* **134**, 2541-2547.
Inoue, K., Ohyama, T., Sakuragi, Y., Yamamoto, R., Inoue, N. A., Li-Hua, Y., Goto, Y. I., Wegner, M. and Lupski, J. R. (2007). Translation of SOX10 3′ untranslated region

causes a complex severe neurocristopathy by generation of a deleterious functional domain. *Hum. Mol. Genet.* **16**, 3037-3046.

Isseroff, R., Grahn, J., Reilly, D. and Nuccitelli, R. (2001). Melanocytes do not exhibit directional migration in a DC electric field. *J. Investig. Dermatol.* **117**, 556.

Iwashita, M., Watanabe, M., Ishii, M., Chen, T., Johnson, S. L., Kurachi, Y., Okada, N. and Kondo, S. (2006). Pigment pattern in jaguar/obelix zebrafish is caused by a Kir7.1 mutation: implications for the regulation of melanosome movement. *PLoS Genet.* **2**, e197.

Iyengar, B. (1998). Photomodulation of the melanocyte cell cycle by indoleamines. *Biol. Signals Recept.* **7**, 345-350.

Jaffe, L. (1982). Developmental currents, voltages, and gradients. In *Developmental Order: its Origin and Regulation* (ed. S. Subtelny), pp. 183-215. New York: Alan R Liss.

Jaffe, L. F. (2003). Epigenetic theories of cancer initiation. *Adv. Cancer Res.* **90**, 209-230.

Jeon, S., Kim, N. H., Koo, B. S., Lee, H. J. and Lee, A. Y. (2007). Bee venom stimulates human melanocyte proliferation, melanogenesis, dendricity and migration. *Exp. Mol. Med.* **39**, 603-613.

Jin, M., Defoe, D. M. and Wondergem, R. (2003). Hepatocyte growth factor/scatter factor stimulates Ca^{2+}-activated membrane K+ current and migration of MDCK II cells. *J. Membr. Biol.* **191**, 77-86.

Kasemeier-Kulesa, J. C., Teddy, J. M., Postovit, L. M., Seftor, E. A., Seftor, R. E., Hendrix, M. J. and Kulesa, P. M. (2008). Reprogramming multipotent tumor cells with the embryonic neural crest microenvironment. *Dev. Dyn.* **237**, 2657-2666.

Kelsh, R. N., Schmid, B. and Eisen, J. S. (2000). Genetic analysis of melanophore development in zebrafish embryos. *Dev. Biol.* **225**, 277-293.

Kim, C. F. and Dirks, P. B. (2008). Cancer and stem cell biology: how tightly intertwined? *Cell Stem Cell* **3**, 147-150.

Konig, S., Hinard, V., Arnaudeau, S., Holzer, N., Potter, G., Bader, C. R. and Bernheim, L. (2004). Membrane hyperpolarization triggers myogenin and myocyte enhancer factor-2 expression during human myoblast differentiation. *J. Biol. Chem.* **279**, 28187-28196.

Kraft, R., Krause, P., Jung, S., Basrai, D., Liebmann, L., Bolz, J. and Patt, S. (2003). BK channel openers inhibit migration of human glioma cells. *Pflugers Arch.* **446**, 248-255.

Kucheryavykh, Y. V., Kucheryavykh, L. Y., Nichols, C. G., Maldonado, H. M., Baksi, K., Reichenbach, A., Skatchkov, S. N. and Eaton, M. J. (2007). Downregulation of Kir4.1 inward rectifying potassium channel subunits by RNAi impairs potassium transfer and glutamate uptake by cultured cortical astrocytes. *Glia* **55**, 274-281.

Kulesa, P. M., Kasemeier-Kulesa, J. C., Teddy, J. M., Margaryan, N. V., Seftor, E. A., Seftor, R. E. and Hendrix, M. J. (2006). Reprogramming metastatic melanoma cells to assume a neural crest cell-like phenotype in an embryonic microenvironment. *Proc. Natl. Acad. Sci. USA* **103**, 3752-3757.

Kumasaka, M., Sato, S., Yajima, I. and Yamamoto, H. (2003). Isolation and developmental expression of tyrosinase family genes in Xenopus laevis. *Pigment Cell Res.* **16**, 455-462.

Kumasaka, M., Sato, H., Sato, S., Yajima, I. and Yamamoto, H. (2004). Isolation and developmental expression of Mitf in Xenopus laevis. *Dev. Dyn.* **230**, 107-113.

Kumasaka, M., Sato, S., Yajima, I., Goding, C. R. and Yamamoto, H. (2005). Regulation of melanoblast and retinal pigment epithelium development by Xenopus laevis Mitf. *Dev. Dyn.* **234**, 523-534.

Kunzelmann, K. (2005). Ion channels and cancer. *J. Membr. Biol.* **205**, 159-173.

Kuriyama, S. and Mayor, R. (2008). Molecular analysis of neural crest migration. *Philos. Trans. R. Soc. Lond. B. Biol. Sci.* **363**, 1349-1362.

Kyrgidis, A., Tzellos, T. G. and Triaridis, S. (2010). Melanoma: Stem cells, sun exposure and hallmarks for carcinogenesis, molecular concepts and future clinical implications. *J. Carcinog.* **9**, 3.

Lastraioli, E., Guasti, L., Crociani, O., Polvani, S., Hofmann, G., Witchel, H., Bencini, L., Calistri, M., Messerini, L., Scatizzi, M. et al. (2004). herg1 gene and HERG1 protein are overexpressed in colorectal cancers and regulate cell invasion of tumor cells. *Cancer Res.* **64**, 606-611.

Lee, L. M., Seftor, E. A., Bonde, G., Cornell, R. A. and Hendrix, M. J. (2005). The fate of human malignant melanoma cells transplanted into zebrafish embryos: assessment of migration and cell division in the absence of tumor formation. *Dev. Dyn.* **233**, 1560-1570.

Lee, M. and Vasioukhin, V. (2008). Cell polarity and cancer-cell and tissue polarity as a non-canonical tumor suppressor. *J. Cell Sci.* **121**, 1141-1150.

Lerchner, W., Xiao, C., Nashmi, R., Slimko, E. M., van Trigt, L., Lester, H. A. and Anderson, D. J. (2007). Reversible silencing of neuronal excitability in behaving mice by a genetically targeted, ivermectin-gated Cl^- channel. *Neuron* **54**, 35-49.

Levens, D. (1990). Development and cancer: common themes? *Lab. Invest.* **63**, 429-431.

Levin, M. (2004). A novel immunohistochemical method for evaluation of antibody specificity and detection of labile targets in biological tissue. *J. Biochem. Biophys. Methods* **58**, 85-96.

Levin, M. (2007). Large-scale biophysics: ion flows and regeneration. *Trends Cell Biol.* **17**, 262-271.

Levin, M. (2009a). Bioelectric mechanisms in regeneration: unique aspects and future perspectives. *Semin. Cell Dev. Biol.* **20**, 543-556.

Levin, M. (2009b). Errors of geometry: regeneration in a broader perspective. *Semin. Cell Dev. Biol.* **20**, 643-645.

Levin, M. and Mercola, M. (1998). Gap junctions are involved in the early generation of left-right asymmetry. *Dev. Biol.* **203**, 90-105.

Levin, M., Buznikov, G. A. and Lauder, J. M. (2006). Of minds and embryos: left-right asymmetry and the serotonergic controls of pre-neural morphogenesis. *Dev. Neurosci.* **28**, 171-185.

Li, C., Zhong, H., Wang, Y., Wang, H., Yang, Z., Zheng, Y., Liu, K. and Liu, Y. (2006). Voltage and ionic regulation of human serotonin transporter in Xenopus oocytes. *Clin. Exp. Pharmacol. Physiol.* **33**, 1088-1092.

Lindvall, C., Bu, W., Williams, B. O. and Li, Y. (2007). Wnt signaling, stem cells, and the cellular origin of breast cancer. *Stem Cell Rev.* **3**, 157-168.

Liu, L. Y., Hu, C. L., Ma, L. J., Zhang, Z. H. and Mei, Y. A. (2004). ET-1 inhibits B-16 murine melanoma cell migration by decreasing K(+) currents. *Cell Motil. Cytoskeleton* **58**, 127-136.

Liu, L. Y., Hoffman, G. E., Fei, X. W., Li, Z., Zhang, Z. H. and Mei, Y. A. (2007). Delayed rectifier outward K^+ current mediates the migration of rat cerebellar granule cells stimulated by melatonin. *J. Neurochem.* **102**, 333-344.

Lotti, T., Gori, A., Zanieri, F., Colucci, R. and Moretti, S. (2008). Vitiligo: new and emerging treatments. *Dermatol. Ther.* **21**, 110-117.

Lund, E. (1947). Bioelectric fields and growth. Austin: Univ. of Texas Press.

Lynch, J. W. (2009). Native glycine receptor subtypes and their physiological roles. *Neuropharmacology* **56**, 303-309.

Macmillan, G. J. (1976). Melanoblast-tissue interactions and the development of pigment pattern in Xenopus larvae. *J. Embryol. Exp. Morphol.* **35**, 463-484.

Makino, S., Whitehead, G. G., Lien, C. L., Kim, S., Jhawar, P., Kono, A., Kawata, Y. and Keating, M. T. (2005). Heat-shock protein 60 is required for blastema formation and maintenance during regeneration. *Proc. Natl. Acad. Sci. USA* **102**, 14599-14604.

Maniotis, A. J., Folberg, R., Hess, A., Seftor, E. A., Gardner, L. M., Pe'er, J., Trent, J. M., Meltzer, P. S. and Hendrix, M. J. (1999). Vascular channel formation by human melanoma cells in vivo and in vitro: vasculogenic mimicry. *Am. J. Pathol.* **155**, 739-752.

McCaig, C. D., Rajnicek, A. M., Song, B. and Zhao, M. (2005). Controlling cell behavior electrically: current views and future potential. *Physiol. Rev.* **85**, 943-978.

McCaig, C. D., Song, B. and Rajnicek, A. M. (2009). Electrical dimensions in cell science. *J. Cell Sci.* **122**, 4267-4276.

Moran, D. (1991). Voltage-dependent -L-type Ca^{2+} channels participate in regulating neural crest migration and differentiation. *Am. J. Anat.* **192**, 14-22.

Morokuma, J., Blackiston, D., Adams, D. S., Seebohm, G., Trimmer, B. and Levin, M. (2008). Modulation of potassium channel function confers a hyperproliferative invasive phenotype on embryonic stem cells. *Proc. Natl. Acad. Sci. USA* **105**, 16608-16613.

Mu, D., Chen, L., Zhang, X., See, L. H., Koch, C. M., Yen, C., Tong, J. J., Spiegel, L., Nguyen, K. C., Servoss, A. et al. (2003). Genomic amplification and oncogenic properties of the KCNK9 potassium channel gene. *Cancer Cell* **3**, 297-302.

Munaron, L., Antoniotti, S., Fiorio Pla, A. and Lovisolo, D. (2004a). Blocking Ca^{2+} entry: a way to control cell proliferation. *Curr. Med. Chem.* **11**, 1533-1543.

Munaron, L., Antoniotti, S. and Lovisolo, D. (2004b). Intracellular calcium signals and control of cell proliferation: how many mechanisms? *J. Cell Mol. Med.* **8**, 161-168.

Nebigil, C. G., Launay, J. M., Hickel, P., Tournois, C. and Maroteaux, L. (2000). 5-hydroxytryptamine 2B receptor regulates cell-cycle progression: cross-talk with tyrosine kinase pathways. *Proc. Natl. Acad. Sci. USA* **97**, 2591-2596.

Nieuwkoop, P. D. and Faber, J. (1967). *Normal Table of Xenopus laevis (Daudin)*. Amsterdam: North-Holland Publishing Company.

Nishiyama, M., von Schimmelmann, M. J., Togashi, K., Findley, W. M. and Hong, K. (2008). Membrane potential shifts caused by diffusible guidance signals direct growth-cone turning. *Nat. Neurosci.* **11**, 762-771.

Nozue, A. T. and Ono, S. (1991). Effects of catecholamine and serotonin in central nervous system in newborn mice with special reference to neural crest cells; presumptive evidence of neural crest origin. *Anatomischer. Anzeiger.* **173**, 147-153.

Nuccitelli, R., Robinson, K. and Jaffe, L. (1986). On electrical currents in development. *BioEssays* **5**, 292-294.

Olivotto, M., Arcangeli, A., Carla, M. and Wanke, E. (1996). Electric fields at the plasma membrane level: a neglected element in the mechanisms of cell signalling. *BioEssays* **18**, 495-504.

Ottesen, E. A. and Campbell, W. C. (1994). Ivermectin in human medicine. *J. Antimicrob. Chemother.* **34**, 195-203.

Ouadid-Ahidouch, H. and Ahidouch, A. (2008). K^+ channel expression in human breast cancer cells: involvement in cell cycle regulation and carcinogenesis. *J. Membr. Biol.* **221**, 1-6.

Ouwerkerk, R., Jacobs, M. A., Macura, K. J., Wolff, A. C., Stearns, V., Mezban, S. D., Khouri, N. F., Bluemke, D. A. and Bottomley, P. A. (2007). Elevated tissue sodium

concentration in malignant breast lesions detected with non-invasive 23Na MRI. *Breast Cancer Res. Treat.* **106**, 151-160.

Oviedo, N. J. and Beane, W. S. (2009). Regeneration: the origin of cancer or a possible cure? *Semin. Cell Dev. Biol.* **20**, 557-564.

Pardo, L. A., del Camino, D., Sanchez, A., Alves, F., Bruggemann, A., Beckh, S. and Stuhmer, W. (1999). Oncogenic potential of EAG K(+) channels. *EMBO J.* **18**, 5540-5547.

Park, P. C., Selvarajah, S., Bayani, J., Zielenska, M. and Squire, J. A. (2007). Stem cell enrichment approaches. *Semin. Cancer Biol.* **17**, 257-264.

Pfeifer, A. and Verma, I. M. (2001). Gene therapy: promises and problems. *Annu. Rev. Genomics Hum. Genet.* **2**, 177-211.

Pogge v Strandmann, E., Senkel, S. and Ryffel, G. U. (2000). Ectopic pigmentation in Xenopus in response to DCoH/PCD, the cofactor of HNF1 transcription factor/pterin-4alpha-carbinolamine dehydratase. *Mech. Dev.* **91**, 53-60.

Potier, M., Joulin, V., Roger, S., Besson, P., Jourdan, M. L., Leguennec, J. Y., Bougnoux, P. and Vandier, C. (2006). Identification of SK3 channel as a new mediator of breast cancer cell migration. *Mol. Cancer Ther.* **5**, 2946-2953.

Prevarskaya, N., Zhang, L. and Barritt, G. (2007). TRP channels in cancer. *Biochim. Biophys. Acta* **1772**, 937-946.

Pullar, C. E., Baier, B. S., Kariya, Y., Russell, A. J., Horst, B. A., Marinkovich, M. P. and Isseroff, R. R. (2006). beta4 integrin and epidermal growth factor coordinately regulate electric field-mediated directional migration via Rac1. *Mol. Biol. Cell* **17**, 4925-4935.

Rajnicek, A. M., Foubister, L. E. and McCaig, C. D. (2006). Growth cone steering by a physiological electric field requires dynamic microtubules, microfilaments and Rac-mediated filopodial asymmetry. *J. Cell Sci.* **119**, 1736-1745.

Reid, B., Nuccitelli, R. and Zhao, M. (2007). Non-invasive measurement of bioelectric currents with a vibrating probe. *Nat. Protoc.* **2**, 661-669.

Reya, T., Morrison, S. J., Clarke, M. F. and Weissman, I. L. (2001). Stem cells, cancer, and cancer stem cells. *Nature* **414**, 105-111.

Robinson, K. R. and Messerli, M. A. (1996). Electric embryos: the embryonic epithelium as a generator of developmental information. In *Nerve Growth and Guidance* (ed. C. D. McCaig), pp. 131-150. London: Portland Press.

Rubin, H. (1985). Cancer as a dynamic developmental disorder. *Cancer Res.* **45**, 2935-2942.

Rubin, H. (1990). The significance of biological heterogeneity. *Cancer and Metastasis Rev.* **9**, 1-20.

Saka, Y. and Smith, J. C. (2001). Spatial and temporal patterns of cell division during early Xenopus embryogenesis. *Dev. Biol.* **229**, 307-318.

Sanchez Alvarado, A. (2003). The freshwater planarian Schmidtea mediterranea: embryogenesis, stem cells and regeneration. *Curr. Opin. Genet. Dev.* **13**, 438-444.

Sauka-Spengler, T. and Bronner-Fraser, M. (2008). A gene regulatory network orchestrates neural crest formation. *Nat. Rev. Mol. Cell Biol.* **9**, 557-568.

Schlosser, G., Awtry, T., Brugmann, S. A., Jensen, E. D., Neilson, K., Ruan, G., Stammler, A., Voelker, D., Yan, B., Zhang, C. et al. (2008). Eya1 and Six1 promote neurogenesis in the cranial placodes in a SoxB1-dependent fashion. *Dev. Biol.* **320**, 199-214.

Schwab, A., Reinhardt, J., Schneider, S. W., Gassner, B. and Schuricht, B. (1999). K(+) channel-dependent migration of fibroblasts and human melanoma cells. *Cell Physiol. Biochem.* **9**, 126-132.

Seagar, M. J., Granier, C. and Couraud, F. (1984). Interactions of the neurotoxin apamin with a Ca^{2+}-activated K^+ channel in primary neuronal cultures. *J. Biol. Chem.* **259**, 1491-1495.

Shan, Q., Haddrill, J. L. and Lynch, J. W. (2001). Ivermectin, an unconventional agonist of the glycine receptor chloride channel. *J. Biol. Chem.* **276**, 12556-12564.

Sive, H. L., Grainger, R. M. and Harland, R. M. (2000). *Early Development of Xenopus Laevis.* New York: Cold Spring Harbor Laboratory Press.

Slominski, A., Tobin, D. J., Shibahara, S. and Wortsman, J. (2004). Melanin pigmentation in mammalian skin and its hormonal regulation. *Physiol. Rev.* **84**, 1155-1228.

Slominski, A., Wortsman, J. and Tobin, D. J. (2005). The cutaneous serotoninergic/melatoninergic system: securing a place under the sun. *FASEB J.* **19**, 176-194.

Song, B., Gu, Y., Pu, J., Reid, B., Zhao, Z. and Zhao, M. (2007). Application of direct current electric fields to cells and tissues in vitro and modulation of wound electric field *in vivo*. *Nat. Protoc.* **2**, 1479-1489.

Soto, A. M. and Sonnenschein, C. (2004). The somatic mutation theory of cancer: growing problems with the paradigm? *BioEssays* **26**, 1097-1107.

Spitzner, M., Ousingsawat, J., Scheidt, K., Kunzelmann, K. and Schreiber, R. (2007). Voltage-gated K^+ channels support proliferation of colonic carcinoma cells. *FASEB J.* **21**, 35-44.

Stahelin, B. J., Marti, U., Solioz, M., Zimmermann, H. and Reichen, J. (1998). False positive staining in the TUNEL assay to detect apoptosis in liver and intestine is caused by endogenous nucleases and inhibited by diethyl pyrocarbonate. *Mol. Pathol.* **51**, 204-208.

Stulberg, D. L., Clark, N. and Tovey, D. (2003). Common hyperpigmentation disorders in adults: Part II. Melanoma, seborrheic keratoses, acanthosis nigricans, melasma, diabetic dermopathy, tinea versicolor, and postinflammatory hyperpigmentation. *Am. Fam. Physician* **68**, 1963-1968.

Stump, R. F. and Robinson, K. R. (1983). Xenopus neural crest cell migration in an applied electrical field. *J. Cell Biol.* **97**, 1226-1233.

Sun, W., Buzanska, L., Domanska-Janik, K., Salvi, R. J. and Stachowiak, M. K. (2005). Voltage-sensitive and ligand-gated channels in differentiating neural stem-like cells derived from the nonhematopoietic fraction of human umbilical cord blood. *Stem Cells* **23**, 931-945.

Sundelacruz, S., Levin, M. and Kaplan, D. L. (2008). Membrane potential controls adipogenic and osteogenic differentiation of mesenchymal stem cells. *PLoS ONE* **3**, e3737.

Sundelacruz, S., Levin, M. and Kaplan, D. L. (2009). Role of membrane potential in the regulation of cell proliferation and differentiation. *Stem. Cell Rev. Rep.* **5**, 231-246.

Taipale, J. and Beachy, P. A. (2001). The Hedgehog and Wnt signalling pathways in cancer. *Nature* **411**, 349-354.

Tan, B. T., Park, C. Y., Ailles, L. E. and Weissman, I. L. (2006). The cancer stem cell hypothesis: a work in progress. *Lab. Invest.* **86**, 1203-1207.

Tang, Y. B., Liu, Y. J., Zhou, J. G., Wang, G. L., Qiu, Q. Y. and Guan, Y. Y. (2008). Silence of ClC-3 chloride channel inhibits cell proliferation and the cell cycle via G/S phase arrest in rat basilar arterial smooth muscle cells. *Cell Prolif.* **41**, 775-785.

Tataria, M., Perryman, S. V. and Sylvester, K. G. (2006). Stem cells: tissue regeneration and cancer. *Semin. Pediatr. Surg.* **15**, 284-292.

Thomas, C. E., Ehrhardt, A. and Kay, M. A. (2003). Progress and problems with the use of viral vectors for gene therapy. *Nat. Rev. Genet.* **4**, 346-358.

Tomlinson, M. L., Garcia-Morales, C., Abu-Elmagd, M. and Wheeler, G. N. (2008). Three matrix metalloproteinases are required in vivo for macrophage migration during embryonic development. *Mech. Dev.* **125**, 1059-1070.

Tomlinson, M. L., Guan, P., Morris, R. J., Fidock, M. D., Rejzek, M., Garcia-Morales, C., Field, R. A. and Wheeler, G. N. (2009a). A chemical genomic approach identifies matrix metalloproteinases as playing an essential and specific role in Xenopus melanophore migration. *Chem. Biol.* **16**, 93-104.

Tomlinson, M. L., Rejzek, M., Fidock, M., Field, R. A. and Wheeler, G. N. (2009b). Chemical genomics identifies compounds affecting Xenopus laevis pigment cell development. *Mol. Biosyst.* **5**, 376-384.

Tseng, A. S., Adams, D. S., Qiu, D., Koustubhan, P. and Levin, M. (2007). Apoptosis is required during early stages of tail regeneration in Xenopus laevis. *Dev. Biol.* **301**, 62-69.

Tucker, R. P. (2004). Neural crest cells: a model for invasive behavior. *Int. J. Biochem. Cell Biol.* **36**, 173-177.

Tung, J. J., Hobert, O., Berryman, M. and Kitajewski, J. (2009). Chloride intracellular channel 4 is involved in endothelial proliferation and morphogenesis in vitro. *Angiogenesis* **12**, 209-220.

Uzman, J. A., Patil, S., Uzgare, A. R. and Sater, A. K. (1998). The role of intracellular alkalinization in the establishment of anterior neural fate in Xenopus. *Dev. Biol.* **193**, 10-20.

van de Veerdonk, F. C. G. (1960). Serotonin, a melanocyte-stimulating component in the dorsal skin secretion of Xenopus laevis. *Nature* **187**, 948-949.

van Kempen, M., van Ginneken, A., de Grijs, I., Mutsaers, N., Opthof, T., Jongsma, H. and van der Heyden, M. (2003). Expression of the electrophysiological system during murine embryonic stem cell cardiac differentiation. *Cell Physiol. Biochem.* **13**, 263-270.

Varnum-Finney, B., Xu, L., Brashem-Stein, C., Nourigat, C., Flowers, D., Bakkour, S., Pear, W. S. and Bernstein, I. D. (2000). Pluripotent, cytokine-dependent, hematopoietic stem cells are immortalized by constitutive Notch1 signaling. *Nat. Med.* **6**, 1278-1281.

Waddington, C. H. (1935). Cancer and the theory of organisers. *Nature* **135**, 606-608.

Watanabe, M., Iwashita, M., Ishii, M., Kurachi, Y., Kawakami, A., Kondo, S. and Okada, N. (2006). Spot pattern of leopard Danio is caused by mutation in the zebrafish connexin41.8 gene. *EMBO Rep.* **7**, 893-897.

Welsch, T., Kleeff, J. and Friess, H. (2007). Molecular pathogenesis of pancreatic cancer: advances and challenges. *Curr. Mol. Med.* **7**, 504-521.

White, R. M. and Zon, L. I. (2008). Melanocytes in development, regeneration, and cancer. *Cell Stem Cell* **3**, 242-252.

Whitton, M. E., Ashcroft, D. M. and Gonzalez, U. (2008). Therapeutic interventions for vitiligo. *J. Am. Acad. Dermatol.* **59**, 713-717.

Wicha, M. S., Liu, S. and Dontu, G. (2006). Cancer stem cells: an old idea-a paradigm shift. *Cancer Res* **66**, 1883-1890; discussion 1895-1896.

Wissenbach, U., Niemeyer, B., Himmerkus, N., Fixemer, T., Bonkhoff, H. and Flockerzi, V. (2004). TRPV6 and prostate cancer: cancer growth beyond the prostate correlates with increased TRPV6 Ca^{2+} channel expression. *Biochem. Biophys. Res. Commun.* **322**, 1359-1363.

Wu, W. K., Li, G. R., Wong, T. M., Wang, J. Y., Yu, L. and Cho, C. H. (2008). Involvement of voltage-gated K^+ and Na^+ channels in gastric epithelial cell migration. *Mol. Cell. Biochem.* **308**, 219-226.

Yamamura, H., Ugawa, S., Ueda, T., Morita, A. and Shimada, S. (2008a). TRPM8 activation suppresses cellular viability in human melanoma. *Am. J. Physiol. Cell Physiol.* **295**, C296-C301.

Yamamura, H., Ugawa, S., Ueda, T. and Shimada, S. (2008b). Expression analysis of the epithelial Na^+ channel delta subunit in human melanoma G-361 cells. *Biochem. Biophys. Res. Commun.* **366**, 489-492.

Yu, S. Y., Yoo, S. J., Yang, L., Zapata, C., Srinivasan, A., Hay, B. A. and Baker, N. E. (2002). A pathway of signals regulating effector and initiator caspases in the developing Drosophila eye. *Development* **129**, 3269-3278.

Zhang, Y. and Levin, M. (2009). Particle tracking model of electrophoretic morphogen movement reveals stochastic dynamics of embryonic gradient. *Dev. Dyn.* **238**, 1923-1935.

Zhao, M., Song, B., Pu, J., Wada, T., Reid, B., Tai, G., Wang, F., Guo, A., Walczysko, P., Gu, Y. et al. (2006). Electrical signals control wound healing through phosphatidylinositol-3-OH kinase-gamma and PTEN. *Nature* **442**, 457-460.